Molecular Cell, Vol. 18, 519–531, May 27, 2005, Copyright ©2005 by Elsevier Inc. DOI 10.1016/j.molcel.2005.04.019

#2192

Phosphatidylinositol-(4,5)-Bisphosphate Regulates Sorting Signal Recognition by the Clathrin-Associated Adaptor Complex AP2

Stefan Höning,[1,6,*] Doris Ricotta,[2] Michael Krauss,[3] Kira Späte,[1,6] Barbara Spolaore,[5] Alison Motley,[4] Margaret Robinson,[4] Carol Robinson,[5] Volker Haucke,[3] and David J. Owen[4,*]

[1]Institute for Biochemistry II
University of Göttingen
Heinrich-Düker-Weg 12
37073 Göttingen
Germany

[2]Department of Biomedical Science and Biotechnology
University of Brescia
Via Valsabbina 19
25124 Brescia
Italy

[3]Institute of Chemistry-Biochemistry
Freie Universität Berlin
Takustrasse 6
14195 Berlin
Germany

[4]Department of Clinical Biochemistry
Cambridge Institute for Medical Research
University of Cambridge
Hills Road
Cambridge, CB2 2XY
United Kingdom

[5]Department of Chemistry
University of Cambridge
Lensfield Road
Cambridge, CB2 1EW
United Kingdom

Summary

The α,β2,μ2,σ2 heterotetrameric AP2 complex is recruited exclusively to the phosphatidylinositol-4,5-bisphosphate (PtdIns4,5P_2)-rich plasma membrane where, amongst other roles, it selects motif-containing cargo proteins for incorporation into clathrin-coated vesicles. Unphosphorylated and μ2Thr156-monophosphorylated AP2 mutated in their αPtdIns4,5P_2, μ2PtdIns4,5P_2, and μ2Yxxϕ binding sites were produced, and their interactions with membranes of different phospholipid and cargo composition were measured by surface plasmon resonance. We demonstrate that recognition of Yxxϕ and acidic dileucine motifs is dependent on corecognition with PtdIns4,5P_2, explaining the selective recruitment of AP2 to the plasma membrane. The interaction of AP2 with PtdIns4,5P_2/Yxxϕ-containing membranes is two step: initial recruitment via the αPtdIns4,5P_2 site and then stabilization through the binding of μ2Yxxϕ and μ2PtdIns4,5P_2 sites to their ligands. The second step is facilitated by a conformational change favored by μ2Thr156 phosphorylation. The binding of AP2 to acidic-dileucine motifs occurs at a different site from Yxxϕ binding and is not enhanced by μ2Thr156 phosphorylation.

*Correspondence: shoening@uni-koeln.de (S.H.); djo30@cam.ac.uk (D.O.)

[6]Present address: Institute for Biochemistry I, University of Cologne, Joseph-Stelzmann-Strasse 52, 50931 Cologne, Germany.

Introduction

During the earliest stage of clathrin-coated vesicle (CCV) formation from various different cellular membranes, transmembrane proteins destined for incorporation into vesicles become concentrated into a region of the membrane coated on its cytosolic face with a polyhedral clathrin lattice. The coat progressively invaginates, finally budding off into the cytoplasm where it is subsequently uncoated and transported to and then fuses with its target compartment. Clathrin is unable to bind directly to either phospholipid or integral protein components of the membrane itself. The mechanical clathrin scaffold of CCVs is linked to the membrane by a diverse set of proteins termed "clathrin adaptors." These can be broadly classified into two types: those that link clathrin to phospholipid components of membranes such as AP180/CALM and the amphiphysins and those that, in addition to binding to clathrin and either a phospholipid and/or a small Arf-like GTPase embedded in the membrane, also recognize transmembrane protein cargo (Traub, 2003). Some cargo binding clathrin adaptors such as the AP complexes (AP1, AP2, AP3, and AP4) and the Golgi-localized γ-ear containing Arf-binding proteins (GGAs) interact with short canonical peptide motifs that are found on a large number of different cargo proteins, whereas other adaptors specifically recognize only a few closely related cargo molecules such as ARH and Dab2 that bind to members of the LDL receptor family, epsinR that binds vti1b, and the arrestins that recognize G protein-coupled receptors (GPCRs) (for review see Owen et al. [2004] and references therein). Cargo can also be bound through the recognition of ubiquitin molecules that have been reversibly attached to lysine side chains of cargo by ubiquitin binding clathrin adaptors such as epsins 1, 2, and 3 and the GGAs (Hicke and Dunn, 2003).

The AP2 adaptor complex is the major cargo clathrin adaptor in endocytic CCVs, being the second most abundant protein after clathrin itself. The AP2 complex is comprised of two large subunits (α and β2), a medium subunit (μ2), and a small subunit (σ2) (reviewed in Owen et al. [2004]). The large subunits can be subdivided into a trunk (70–75 kDa) and an appendage domain (~30 kDa) joined by an extended, proteolytically-sensitive flexible linker. Under the electron microscope, the AP2 complex appears as a large central core (consisting of the α and β2 trunks and the entire μ2 and σ2 subunits) flanked by two smaller appendages. AP2 interacts with the plasma membrane PtdIns4,5P_2 at two basic sites on the α and μ2 subunits (Gaidarov et al., 1996; Rohde et al., 2002) and directly with clathrin through an Lϕxϕ[DE] clathrin box, which is

found in the β2 hinge. AP2 is also able to interact with other clathrin adaptors as well as with proteins presumed to play accessory roles in endocytic vesicle formation, including Eps15, amphiphysin, auxilin, synaptojanin, stonins, NECAPs, and the protein kinase AAK1 (α-adaptin-associated kinase 1). AP2 achieves this through the binding of its appendages to DPF, FxDxF, and WxxF motifs found in long unstructured regions of these proteins (Owen et al., 2004; Praefcke et al., 2004). AP2 has been shown to bind to protein cargo through Yxxϕ-sorting motifs via the C-terminal subdomain of its μ2 subunit (C-μ2, residues 157–435) (Ohno et al., 1995; Owen and Evans, 1998). The binding to acidic dileucine motifs is a point of contention in the literature. It has been variously suggested that AP2 binds D/ExxxLL acidic sorting motifs through its β2 subunit (Rapoport et al., 1998), its μ2 subunit (Rodionov and Bakke, 1998), and also that AP2 does not bind to acidic dileucine motifs at all (Janvier et al., 2003).

The structure of the entire AP2 core complexed with the PtdIns4,5P_2 homolog D-myo-inositol-hexakisphosphate (IP6) revealed that a conformational state exists that is unable to bind Yxxϕ motifs due to blocking of its binding site on μ2 by portions of the β2 subunit (Collins et al., 2002; Figure 1A). In this conformation, the elongated all β sheet C-μ2 subdomain sits in a spatially complementary shallow groove made by the other subunits. It has also been shown that AP2 can be phosphorylated on a single threonine residue in the linker between the two domains of μ2 (Thr156) by the clathrin-activated AAK1 (Conner and Schmid, 2002; Jackson et al., 2003) and that this event is required for sequestration of transferrin into coated pits (Olusanya et al., 2001) through increased binding to membranes containing endocytic cargo proteins (Ricotta et al., 2002). As a result of these data, a model can be proposed in which AP2 has at least two conformational states: one "closed" and unable to bind Yxxϕ motif-containing cargo and therefore "inactive" (structure determined) and at least one "open" conformation that is able to bind Yxxϕ motifs. The transition from inactive to active would be favored by μ2Thr156 phosphorylation and juxtaposition of the complex to the PtdIns4,5P_2-containing plasma membrane. A similar model has recently been proposed on the basis of biochemical and cell biological data for the functioning of the AP1 complex (Ghosh and Kornfeld, 2003; Heldwein et al., 2004). In this case, the role of PtdIns4,5P_2 would presumably be assumed by PtdIns4P, which has recently been shown to be important for the binding of AP1 to the Golgi (Wang et al., 2003); however, the identity of the kinase responsible for phosphorylating the μ1 subunit is unclear (Umeda et al., 2000).

Here, we examine the binding of wild-type (wt) and mutant forms of phosphorylated and nonphosphorylated AP2 cores (mutated in the PtdIns4,5P_2 and Yxxϕ binding sites) to "membrane mimics" (i.e., phospholipid liposomes containing various phosphatidyl inositol polyphosphates [PIPs] and/or protein cargo-sorting signals) by using surface plasmon resonance. The data presented show that recombinant AP2 does indeed bind directly to acidic dileucine motifs as well as to Yxxϕ motifs and that the binding to the two different motifs occurs at nonoverlapping sites. We also demonstrate that the interaction of AP2 with a PtdIns4,5P_2/Yxxϕ cargo-containing membrane is a two-step mechanism: an initial weak binding to PtdIns4,5P_2 via the α subunit, followed by a conformational change favored by μ2Thr156 phosphorylation that allows simultaneous binding of the Yxxϕ motif and further PtdIns4,5P_2 at sites both on the μ2 subunit. This conformational change does not, however, increase binding to acidic dileucine motifs. Most importantly, recognition of both types of signal only occurs when the cargo is displayed in a membrane containing phosphoinositides and is of highest affinity if PtdIns4,5P_2 is present, thus explaining the exclusivity of the subcellular localization of AP2 to the plasma membrane despite the presence of AP2 cargo on other intracellular membranes.

Results

Characterization of Recombinant Phosphorylated AP2

Recent studies on the function of AP2 have demonstrated that phosphorylation of the AP2 μ2 subunit modulates its function, with phosphorylation being a trigger for high-affinity binding of tyrosine-based sorting signals (Ricotta et al., 2002). A drawback of these in vitro studies was that they used AP2 complexes purified from intact tissue in the presence of high concentrations of Tris, which is known to be partly chaotropic. More importantly, these AP2 preparations can be contaminated with other components of the endocytic machinery, including accessory proteins such as protein kinases (AAK1 and GAK; Conner and Schmid, 2002; Ricotta et al., 2002). The presence of CCV-associated kinases and phosphatases, as well as of other kinases and phosphatases liberated during the initial steps of CCV isolation from tissue, make it very hard to estimate the degree and position of AP2 phosphorylation sites. In order to assess the differences in properties between unphosphorylated AP2 complexes and those stoichometrically phosphorylated on μ2 at Thr156, the site which is phosphorylated in vivo by AAK1 (Pauloin and Thurieau, 1993; Olusanya et al., 2001; Ricotta et al., 2002), we have established a method to produce recombinant AP2 cores phosphorylated with a high degree of efficiency on this site. Phosphorylated AP2 cores were made by coexpressing the kinase domain (residues 1–325) of the μ2 kinase AAK1 (gift of Dr. E. Smythe) along with the other four subunits of AP2 core in *E. coli*. (see Experimental Procedures). By SDS-PAGE, phosphorylated and nonphosphorylated AP2 cores (referred to as P-Core and Core, respectively, throughout the manuscript) looked identical, and no AAK1 kinase domain was detected bound to the phosphorylated cores (Figure 1B).

Core and P-Core, purified as in Collins et al. (2002), were subjected to analysis by various mass spectrometry techniques in order to determine their degree of phosphorylation. Nanoflow electrospray mass spectrometry under conditions that preserve noncovalent interactions showed that both the phosphorylated and unphosphorylated complexes were stable and intact, indicating that the phosphorylation does not impair the stability of the complex. The phosphorylated AP2 core

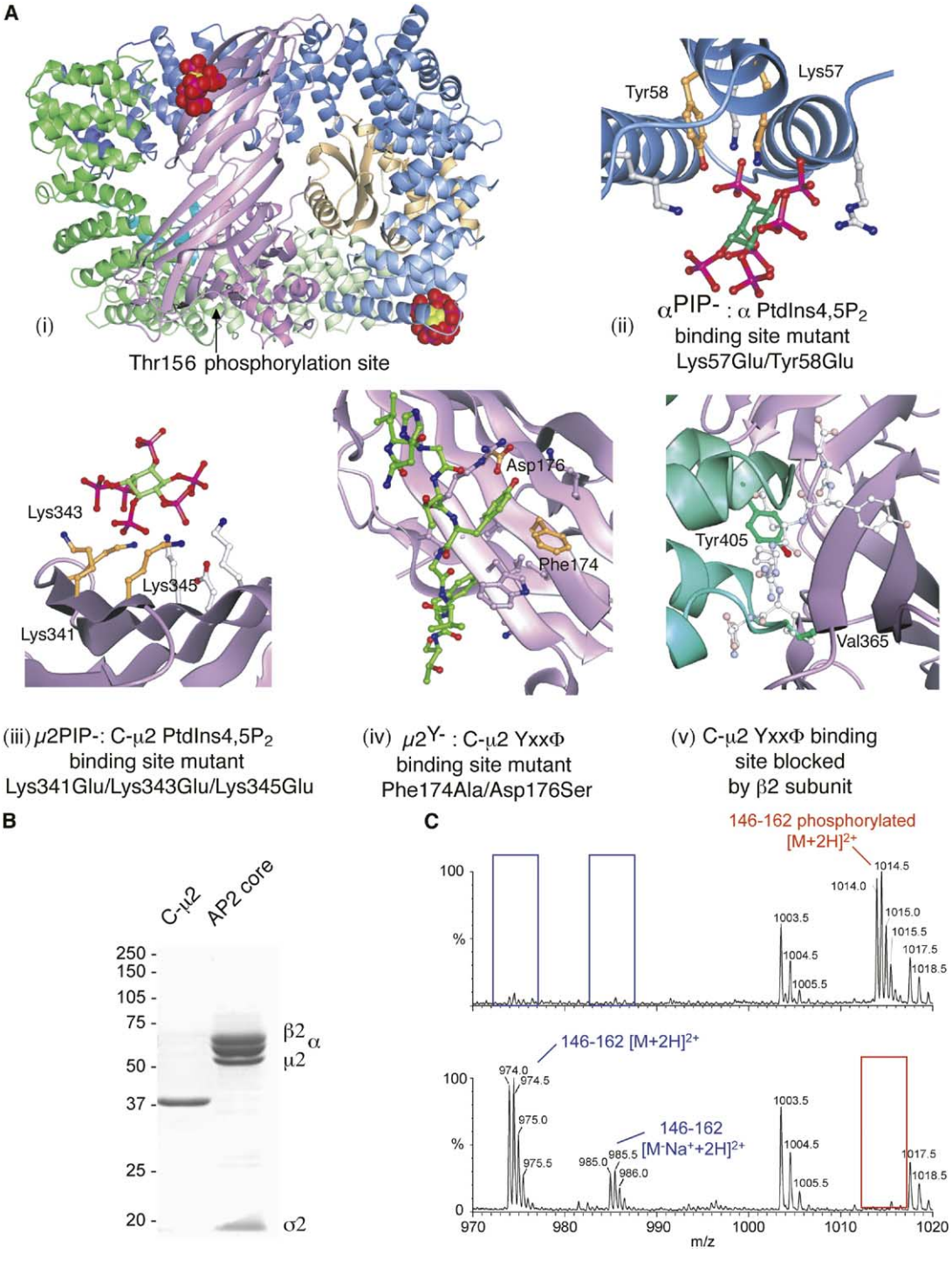

Figure 1. Structure and Phosphorylation of Recombinant AP2 Cores

(A) Functionally important binding sites of AP2. (i) The structure of the whole AP2 complex colored by subunit (α, blue; β2, green; μ2, purple; and σ2, gold). The site of phosphorylation by AAK1 on μ2 Thr156 is indicated, although the actual 12 amino acid segment on which it occurs is invisible in the structure's electron density. Bound IP6 molecules are shown in space-filling representation with carbon colored green, oxygen colored red, and phosphorous colored magenta. (ii–iv) Details of PtdIns4,5P_2 and Yxxϕ binding sites with residues mutated to abolish binding function shown in gold. (v) Yxxϕ binding site blocked by portions of the β2 subunit. The Yxxϕ peptide, in the position in which it should bind, is shown in gray.

(B) SDS-PAGE analysis of μ2 and AP2 core The purity and composition of all AP2 core complexes, and recombinant C-μ2 was verified by SDS-PAGE. A representative Coomassie-stained gel with C-μ2 (20 μg) and the nonphosphorylated AP2 core (60 μg) is shown.

(C) Nanoelectrospray mass spectra of the tryptic digests of the phosphorylated and nonphosphorylated AP2 complex. Mass spectra of the tryptic digest of AP2 phosphorylated (top) and nonphosphorylated (bottom). The regions of the mass spectra of the μ2 tryptic peptide 146–162 are shown. The position corresponding to where the unphosphorylated peptide should run is shown boxed in blue, and where the phosphorylated peptide should run is boxed in red. The m/z values of the peptide in the two mass spectra are indicated, and they correspond to the double charge species. The identity of each peptide was confirmed by MS/MS (see Supplemental Data).

complex gave the spectrum shown in Figure S1A (available in the Supplemental Data with this article online). Only one charge state series is present centered at 7000 m/z, which corresponds to a mass of 206,148.6 Da with a difference only of the 0.08% from the theoretical mass of 205,989.8 Da. Analysis of acid-dissociated P-Core subunits showed that, although the α, β2, and σ2 subunits had masses very close to their theoretical masses, the μ2 subunit has a molecular mass ~80 Da higher than its theoretical unphosphorylated mass (measured mass for phospho-μ2 = 51,055.4; predicted phospho-μ2 = 51,051.3), indicating the addition of a single phosphate group per μ2 (Figure S1B). The MS/MS sequence analysis of tryptic digests of the P-Core and Core demonstrated that phosphorylation occurred in the tryptic peptide 146–162, and furthermore, from studying the fragmentation patterns, it was shown that there was only one site of phosphorylation corresponding to Thr156, which is the site of in vivo phosphorylation by AAK1 (see Figures S1C and S1D). Analysis of the signal intensities for the 146–162 tryptic peptide from P-Core and Core indicated that the efficiency of phosphorylation was greater than 95% (see Supplemental Data).

Recombinant AP2 Core Complexes Bind Sorting Signals

In order to verify the suitability of recombinant Core and P-Core for functional studies, we used surface plasmon resonance (SPR) to compare their binding to the tyrosine-based signal from TGN38 (DYQRLN) immobilized on carboxy-methylated dextran sensorchip (CM5) surfaces with that of native AP2 isolated from porcine brain and recombinant bacterially expressed C-μ2 (residues 157–435) where the Yxxϕ binding site is located (Owen and Evans, 1998). The values for the rate constants obtained for all four samples were comparable (see Table S1), and all fitted well to a one to one binding model. Similar strengths of interaction were obtained for binding of the TGN38 sequence DYQRLN to C-μ2 both in solution-based fluorimetric and in isothermal titration calorimetry assays. (D.J.O. and T. Dafforn, unpublished data). P-Core bound with a ~13-fold higher affinity to TGN38 than did unphosphorylated Core (K_Ds were: 36 nM for P-Core and 450 nM for Core). Similar data were obtained by using a number of other tyrosine-based signals (see Supplemental Data). Analysis of the data revealed that the increase in affinity was due to an increase in the "on rate" (k_a), whereas the measured "off rates" (k_d) were in the same range. This is consistent with a model in which phosphorylation favors a conformational change that is required in order to achieve effective Yxxϕ motif cargo binding, i.e., in the case of the phosphorylated complex, less energy is required to affect the conformational change than in the case of the unphosphorylated form, resulting in the Yxxϕ binding competent conformation being more prevalent in the phosphorylated form.

AP2 Binds Weakly to Membranes Containing PtdIns4,5P_2

In the cell, AP2 recognizes cargo motifs in the context of being embedded in a PtdIns4,5P_2-containing phospholipid membrane and not free in aqueous solution. In order to better mimic the in vivo situation, we aimed to reconstitute AP2 binding to membranes in vitro. First, liposomes of different composition were prepared containing either a simple phospholipid mixture (phosphatidyl choline, PC 80%; phosphatidyl ethanolamine, PE 20%) or simple lipids plus one single species of phosphoinositide (70% PC, 20% PE, and 10% PIP). In a liposome "spin-down" assay (see Experimental Procedures), recombinant AP2 bound preferentially to liposomes containing PtdIns4,5P_2 over liposomes containing other PIPs tested (see Figure 2A and also Figure 4A). Quantitation of the liposome pull-down assays showed that approximately twice as much P-Core as Core bound to PtdIns4,5P_2-containing liposomes (Figures 2B and C).

To further confirm the specificity of AP2 for PtdIns4,5P_2 and in order to analyze AP2 binding to membranes with higher sensitivity in real time, we have developed a SPR-based binding assay. Liposomes were injected at a low flow rate over a sensorchip surface containing lipophilic alkyl side chains (L1 chip, Cooper et al., 2000) of a BIAcore 3000 biosensor. The integrity of the liposomes was confirmed by electron microscopy (see Figure 2D, panel i). Coating of the L1 surface with liposomes resulted in a positive shift of the baseline of 9000–10,500 resonance units (RU). After liposome capture, the surface was treated with short pulse injections of sodium hydroxide to remove lipid multilayers or loosely attached liposomes. This resulted in a decrease of the baseline of ~200 RU. Subsequently, the baseline was stable during multiple rounds of protein injection and regeneration. Indeed, when the sensor surface was undocked from the instrument and processed for electron microscopy, intact liposomes could still be observed in cross-sections (Figure 2D, panel ii). This was also confirmed by analysis of the L1 sensor surface by laser-scanning microscopy after immobilization of rhodamine B-filled liposomes (data not shown). We have thus established a membrane mimic assay that allows the real-time detection of molecule binding to captured liposome membranes of defined phospholipid composition (see model depicted in Figure 2D, panel iii).

Because each sensorchip contains four individual flow cells that could be coated with different types of liposomes, the membrane mimic assay allows simultaneous comparison of AP2 binding to four different types of membranes. Monitoring AP2 binding in this way revealed a striking specificity of AP2 for membranes containing PtdIns4,5P_2, because we were unable to detect any binding of AP2 to membranes containing phosphatidyl inositide-monophosphates (PtdIns3P, PtdIns4P, and PtdIns5P) nor to PtdIns3,5P_2 (see Figure 4A) above background levels. Binding of the AP2 core to PtdIns4,5P_2 membranes was determined to be weak (K_D = 7.6 μM), but use of the P-Core increased the affinity more than 2-fold (K_D = 2.9 μM as opposed to 7.6 μM, see Table 1), which is consistent with the amounts of AP2 precipitated in the liposome pull-down assay. The observed differences in affinities are largely due to a reduction in k_d. This can be explained if in the conformation favored by μ2Thr156 phosphorylation, both the α and μ2 PtdIns4,5P_2 binding sites can bind simultaneously to a PtdIns4,5P_2-con-

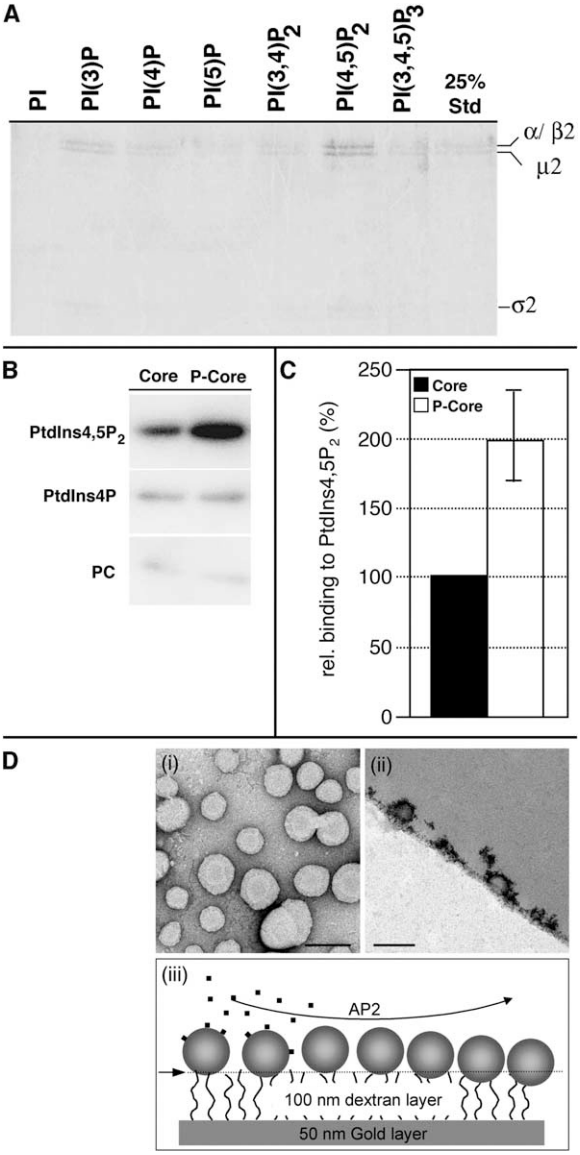

Figure 2. AP2 Binds Selectively to the Phosphoinositide PtdIns(4,5)P_2

(A) AP2 binding to phosphoinositides. Liposomes containing the indicated phospoinositide (10%) were incubated with AP2 core complexes, reisolated, washed, and analyzed by SDS-PAGE and staining with Coomassie blue. 25% Std, 25% of the total AP2 added to the assay.

(B) Phosphorylation enhances AP2 binding to PtdIns(4,5)P_2-containing liposomes. Liposomes comprised of phosphatidylcholine (70%), phosphatidylethanolamine (20%), and PtdIns(4,5)P_2 (10%) were incubated with Core and P-Core complexes, reisolated, washed, and analyzed by SDS-PAGE and immunoblotting for α-adaptin.

(C) Quantification by phosphoimage analysis in (B). Binding of core to PtdIns(4,5)P_2-containing liposomes is shown in black and of P-Core in white. The amount of unphosphorylated Core bound to PtdIns(4,5)P-containing liposomes was taken as 100%. Data represent the mean ± SD from three independent experiments.

(D) A biosensor-based membrane-mimic assay. To assay the binding of AP2 to membranes in a defined system, liposomes of known composition were immobilized on a L1 sensorchip surface via lipophilic alkyl chain anchors. Liposomes captured in this way provided a chemically and physically stable environment that resembles a cellular membrane, and the gold surface on which the hydrogel is based is suitable for SPR analysis. This assumption was confirmed by electron microscopy. (i) Integrity of the prepared liposomes (average size 100 nm). (ii) Cross-section through an L1 sensor surface after liposome capture and AP2 binding experiments. Intact as well as partially cut liposomes are visible (upper half, dark gray), whereas the dextran matrix itself was not preserved (lower translucent area). (iii) Model showing the proportions that exist during binding of AP2 to liposome membranes captured on a L1 sensor surface. The area above the arrow (left) and the dotted line represent the visible structures in (ii), whereas the dextran matrix below the dotted line could not be imaged. Bars = 0.2 μm.

Table 1. Binding of Recombinant AP2 to PtdIns4,5P_2

	Binding to Ptdins4,5P_2		
	k_a ($M^{-1} \times s^{-1}$)	K_d (s^{-1})	K_d (nM)
Core	0.5×10^3	3.8×10^{-3}	7600
P-Core	0.7×10^3	2.0×10^{-3}	2900
α^{PIP-} Core	ND	ND	ND
α^{PIP-} P-Core	ND	ND	ND
$\mu2^{PIP-}$ Core	0.4×10^3	4.2×10^{-3}	10,500
$\alpha + \mu2^{PIP-}$ P-Core	0.4×10^3	4.4×10^{-3}	11,000

Liposomes with/without PtdIns4,5P_2 were immobilized on a L1 biosensor surface to create a stable membrane mimic environment, then probed for binding of recombinant AP2 and mutants thereof by SPR. Binding to membranes without PtdIns4,5P_2 was regarded as background and subtracted from the sensorgrams before calculation of the rate constants. The data show the existence of two PtdIns4,5P_2 binding sites in AP2 located in α- and μ2-adaptins.

taining membrane, thus increasing the aviditiy of binding (chelate effect), whereas in the closed form, which is favored in the unphosphorylated state, only one site on any one complex can bind to a PtdIns4,5P_2 in the membrane.

Probing the Role of Individual Binding Sites in AP2 through Mutagenesis

The use of recombinant AP2 cores in the membrane mimic binding assay outlined above opened the way for testing the hypotheses of AP2 function through the use of mutant forms of the complex. In order to address the roles of both PtdIns4,5P_2 binding sites and of the Yxxϕ binding site in AP2 function, mutants were generated in all three. The system of coexpression from two plasmids (α and σ2 from one plasmid and β2 and μ2 from a second) allowed for the effect of combinations of different mutants to be readily tested. The mutations were designed on the basis of the structures of the AP2 core (Collins et al., 2002) and the isolated C-μ2 (Owen and Evans, 1998) (see Figure 1A). The PtdIns4,5P_2 binding site on the α subunit was rendered nonfunctional by mutating its two major phosphate-contacting residues Lys57 and Tyr58 to glutamates (AP2$^{\alpha PIP-}$) (Figure 1A, panel ii) and that on the μ2 subunit by mutating Lys341, Lys343, and Lys345 again to glutamate residues (AP2$^{\mu 2PIP-}$) (Figure 1A, panel iii). Yxxϕ motif binding was abrogated by mutating two residues in μ2 involved in binding the tyrosine residue (Phe174 and Asp176) to alanine and serine, respectively (AP2$^{\mu 2Y-}$) (Figure 1A, panel iv). The mutation of these residues has been shown to greatly inhibit the binding of Yxxϕ

peptides to isolated μ2 without affecting μ2 structure in a fluorimetric assay system (D.J.O., unpublished data) and, in the context of intact, AP2 to greatly reduce transferrin receptor internalization (Nesterov et al., 1999). All mutations expressed assembled into complexes, purified similarly and looked identical by SDS-PAGE to wt AP2 cores, and had identical CD spectra (see Figure 1B and data not shown), indicating that the mutations did not affect folding of individual subunits.

When the AP2$^{\alpha PIP-}$ mutant was passed over the PtdIns4,5P_2-containing membranes, binding was as low as that detected for simple lipid membranes, and it was independent of the phosphorylation status of the mutant cores (Table 1). On mutating the PtdIns4,5P_2 binding site in μ2 (AP2$^{\mu 2PIP-}$) in the background of either Core or P-Core, we again observed a decrease in binding to similar levels (10.5 and 11 μM, respectively) (see Table 1). These data suggest that in the absence of the μ2 PtdIns4,5P_2 binding site, the only interaction between AP2 cores and the PtdIns4,5P_2-containing liposomes is through the PtdIns4,5P_2 binding site on α. The finding that mutation of the α site alone was sufficient to abrogate the interaction between AP2 and membranes indicates that this site is pivotal in the initial recruitment. The results further support a model in which the binding sites for PtdIns4,5P_2 on μ2 and the α subunit can "cooperate" to increase the avidity of the binding of AP2 to a PtdIns4,5P_2-containing membrane only in a conformation favored by μ2Thr156 phosphorylation.

AP2 Binds Sorting Signals in the Presence of PtdIns4,5P_2

It is still a matter of debate whether the presence of PtdIns4,5P_2 and a sorting motif-bearing cargo are sufficient for efficient recruitment of AP2 to the cell's limiting membrane. In order to address this question with our assay system, we next compared AP2 core binding to PC/PE-only membranes, membranes containing either PtdIns4,5P_2 or a Yxxϕ-sorting signal (attached to a phosphatidyl ethanolamine backbone, see Experimental Procedures), and to membranes with both PtdIns4,5P_2 and the tyrosine-sorting signal. Negligible binding of Core and P-Core to PC/PE membranes displaying the Yxxϕ motif of TGN38 was detected, but binding was of high affinity when the sorting signal was presented together with PtdIns4,5P_2 (Figure 3A). The binding of P-Core to these latter surfaces was more than 4-fold stronger (K_D = 72 nM) than the binding of core (K_D = 311 nM) (Table 2 and Figure 3A). Evaluation of the binding by using the manufacturer's software indicated that the mode of interaction between the plasma membrane mimic and recombinant AP2 was not a simple one-step process (see Supplemental Data). Instead, the interaction fitted a two-state model, consistent with an initial weak binding event followed by a second step in which the interaction is strengthened. We interpret this as the weak initial association of PtdIns4,5P_2 with a single site on the α subunit, followed by simultaneous binding of a second PtdIns4,5P_2 and Yxxϕ motif-containing cargo to the μ2 subunit. This second step must be energetically more favorable in the phosphorylated form of the complex. On the basis of the AP2 core structure, this would correspond to C-μ2 becoming dislodged from the shallow pocket in which it sits on the surface of AP2.

To further probe the validity of this model, we compared the ability of the phosphorylated and unphosphorylated wt and mutant AP2 cores (α^{PIP-} P-Core, $\mu 2^{PIP-}$ P-Core and $\mu 2^{Y-}$ P-Core, α^{PIP-} Core, and $\mu 2^{PIP-}$ Core and $\mu 2^{Y-}$ Core) to bind to PtdIns4,5P_2/Yxxϕ membrane surfaces. Binding could still be detected for $\mu 2^{Y-}$ P-Core and $\mu 2^{Y-}$ Core (see Figure 3B and Table 2) but was reduced to values comparable to those obtained for binding of wt P-Cores to PtdIns4,5P_2-only membranes. This confirms that AP2 binds Yxxϕ signals at only one site located on the μ2 subunit and the loss of the Yxxϕ binding site had no effect on PtdIns4,5P_2 binding to either Core or P-Core, which confirms the functional independence of these sites (Table 2). Binding of α^{PIP-} P-Core and α^{PIP-} Core were, however, reduced to undetectable background values (PC/PE membrane levels of binding), demonstrating the absolute requirement for the initial α subunit/PtdIns4,5P_2 interaction for subsequent Yxxϕ binding. Mutation of the μ2 PtdIns4,5P_2 binding site weakens the binding of both Core and P-Core to PtdIns4,5P_2/Yxxϕ-containing membranes with the effect being much more pronounced when the mutation is present in a phosphorylated AP2 core background (4-fold reduction, see Table 2). Taken together, these data indicate that the interaction between Yxxϕ and the AP2 μ2 subunit is stronger than that between PtdIns4,5P_2 and μ2, although significant binding to PtdIns4,5P_2 does occur as indicated by experiments in which membrane binding of soluble C-μ2 and a C-μ2 variant with a mutated PtdIns4,5P_2 binding (C-$\mu 2^{PIP-}$) site to a variety of liposomes was analyzed (see Table 2 and Figure 3C). However, the binding of C-μ2 to Yxxϕ/PtdIns4,5P_2-containing membranes was 5-fold tighter than the binding of C-$\mu 2^{PIP-}$, indicating that PtdIns4,5P_2 binding by μ2 stabilizes the membrane interaction of AP2. This is further supported by comparing the binding of C-μ2 to membranes containing the Yxxϕ motif in the presence and absence of PtdIns4,5P_2. This revealed that presence of PtdIns4,5P_2 slowed down the rate of dissociation of C-μ2 from membranes by a factor of four without appreciably affecting the on rate. This is to be expected for a predominantly electrostatic interaction that will decrease rapidly in strength with distance in a high dielectric constant medium, and as a result, such an interaction is unlikely to play a major role in recruiting μ2 to membranes but would help to keep it in the vicinity of the membrane surface once recruited there by another means. The analysis of AP2 core recruitment to membranes in vitro has been carried out at salt concentrations (250 mM NaCl) above physiological ionic strength in order to maintain the cores in a soluble and unaggregated form, and therefore the physiological importance of PtdIns4,5P_2 binding to μ2 has likely been underestimated here, because a purely ionic interaction such as this would be weakened at elevated ionic strengths.

The data presented above show that recognition of protein cargo by AP2 in vitro depends on the cargo being displayed in a PtdIns4,5P_2-containing membrane. This agrees with published in vivo data showing that modifying PtdIns4,5P2 levels in vivo alters rates of endocytosis (Padron et al., 2003; Krauss et al., 2003). In

Table 2. Rate Constants for Binding of Recombinant AP2 and μ2 to Sorting Signals Embedded in a Lipid Environment

	PtdIns4,5P_2 (nM)	PtdIns4,5P_2 + TGN38 (nM)	PtdIns4,5P_2 + CD4^P (nM)
Core	7600	311	930
P-Core	2900	72	910
α^{PIP-} Core	–/–	–/–	–/–
α^{PIP-} P-Core	–/–	–/–	–/–
$\mu2^{PIP-}$ Core	10,500	450	950
$\mu2^{PIP-}$ P-Core	11,000	250	940
α + $\mu2^{PIP-}$ Core	ND	ND	ND
α + $\mu2^{PIP-}$ P-Core	–/–	–/–	–/–
$\mu2^{Y-}$ Core	7200	7000	930
$\mu2^{Y-}$ P-Core	3300	3000	920
C-μ2	?	110	–/–
C-$\mu2^{PIP-}$	–/–	450	–/–

Peptides containing the sorting signals of TGN38 and phosphorylated CD4 were fused to an activatable lipid, incorporated into PtdIns4,5P_2-containing liposomes, and immobilized on a L1 sensor surface as described above. Surfaces containing only PC/PE or PC/PE + PtdIns4,5P_2 served as controls. Recombinant AP2 and μ2 were passed over the surfaces as described in the legends to Figures 4 and 5, and the rate constants were calculated as described. None of the interactions fitted to a simple mathematical model describing a 1:1 type of interaction but rather to a model assuming that AP2 binding to membranes involves multiple binding sites (see also Figure S2). For clarity, only the equilibrium constants are shown. Binding of C-μ2 to PtdIns4,5P_2 was detectable but too weak to permit accurate fitting of the data.

order to further confirm that this is the case in vivo, we have analyzed the PtdIns4,5P_2 dependence of the interaction between AP2 and the epidermal growth factor receptor (EGFR), which under physiological conditions can be internalized in a clathrin/AP2-dependent manner (Huang et al., 2004). COS cells transfected with the EGFR alone or cells transfected with the receptor and an HA-tagged membrane-targeted 5′-phosphatase domain of synaptojanin 1 (HA-IPP-CAAX) were used as a source for coimmunoprecipitation of the EGFR with AP2. Immunoprecipitation of AP2 from cells transfected with the EGFR alone results in efficient coimmunoprecipitation of the EGFR (Sorkin et al., 1996), but, as shown in Figure 3D, coimmunoprecipitation of the EGFR does not occur when cells cotransfected with the EGFR and HA-IPP-CAAX were used in which there are reduced levels of PtdIns4,5P_2 due to overexpression of HA-IPP-CAAX that cleaves the 5′-phosphate group from PtdIns4,5P_2 headgroups (Krauss et al., 2003).

Yxxϕ motif-containing cargo is present in different membranes of the cell as a result of vesicle trafficking; for instance, TGN38 is found mostly on the TGN membranes rather than on the cell's limiting membrane, and yet AP2, which binds to the TGN38 motif more strongly than it does to any other motif, is found exclusively at the plasma membrane (Robinson, 1993). One of the major markers of membrane identity is PIP composition (for review see De Matteis and Godi [2004]), and so in view of this and our data showing that AP2 had a marked preference for PtdIns4,5P_2 over any other PIP when presented in membranes without a Yxxϕ motif (Figure 4A), we next tested how the Yxxϕ motif of TGN38 can be recognized in the context of any other PIP. The data in Figure 4B show that binding of AP2 to the TGN38 signal was detectable when PtdIns3P, PtdIns4P, and PtdIns3,5P_2 were present (680 nM, 650 nM, and 550 nM, respectively). However, binding was much more transient as compared to binding of AP2 to the TGN38 signal in the presence of the mainly plasma membrane-localized PtdIns4,5P_2. The affinity of AP2 cores for PtdIns4,5P_2-containing membranes was consistently 7-fold higher than for any other lipid tested (70 nM, equivalent to other measurements as shown in Figure 4B). In conclusion, we demonstrate that binding of AP2 to membranes containing the tyrosine signal of TGN38 is only stabilized when presented in combination with PtdIns4,5P_2.

AP2 Binds Directly to Acidic Dileucine-Based Sorting Motifs at a Site that Does Not Overlap with the Yxxϕ Binding Site

The data presented so far can explain how AP2 is involved in recognition of tyrosine-sorting motifs of the Yxxϕ type but give no indication as to how or if dileucine motifs are recognized. Data have been presented to show that dileucine motifs are recognized by the adaptor μ chains (Rodionov and Bakke, 1998), which is in apparent contrast to studies that showed binding to the adaptor large subunits (Rapoport et al., 1998). More recent studies (Janvier et al., 2003) have suggested that dileucine motifs do not bind to AP2 at all. These discrepancies may in part be explained by fundamental differences in the methodology used and differences in both sequence and local environment of the dileucine motifs analyzed. Dileucine motifs that function as AP complex-mediated trafficking signals usually conform to the sequence [DE]xxxL[LI] (Bonifacino and Traub, 2003). Others, such as that in CD4, belong to a group of sorting signals that become activated on phosphorylation of serine residues in the vicinity of the double leucine motif and in the case of CD4 then mediate its rapid internalization from the plasma membrane. The phosphorylated residues presumably mimic the acidic residues in the nonphosphorylated signals. We show here that the phosphorylated sequence from CD4 (Pitcher et al., 1999) does not bind to C-μ2 (Figure 5A), whereas it is able to bind to Core and P-Core, as well as the $\mu2^{Y-}$ mutants thereof with equal affinities (Figures 5B and 5C and Table 2, K_Ds of ~900 nM). Binding of AP2 was not restricted to the phosphorylated dileucine signal of CD4 but was also observed for the dileucine signals derived from LIMP-II and tyrosinase. Thus, we demonstrate direct binding of dileucine motifs to AP2 at a site not present on C-μ2, i.e., distinct from and

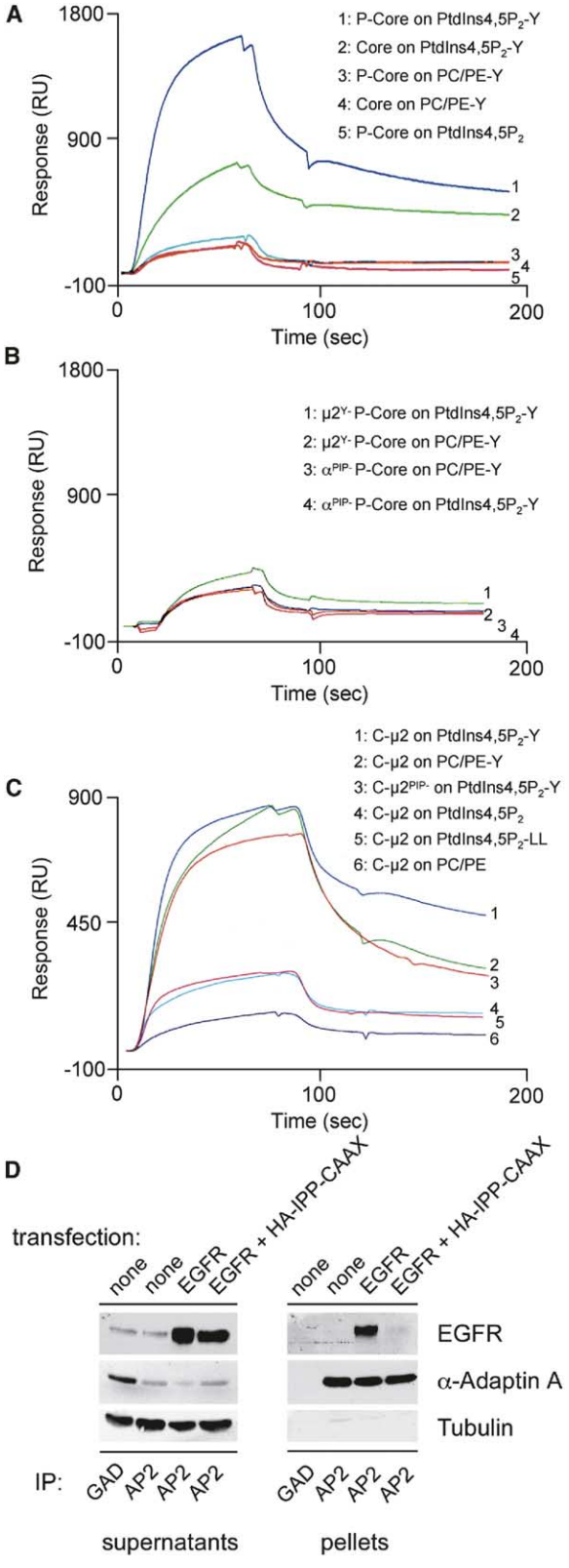

Figure 3. Sorting Signal Binding by AP2 Requires PtdIns(4,5)P_2

(A–C) The four flow cells of a L1 sensorchip were derivatized with liposomes containing PC/PE, with PC/PE + 10% PtdIns(4,5)P_2 (PC/PE-PtdIns4,5$_2$), with PC/PE + 10% of the lipid linked TGN38 tyrosine-sorting signal (PC/PE-Y) and with the same signal in PtdIns(4,5)P_2-containing liposomes (PtdIns4,5$_2$-Y). Subsequently, the surfaces were probed for binding of mutant AP2 cores and C-μ2 as indicated. (A) The sensorgrams of Core (curves 2 and 4) and P-Core (curves 1 and 3) show that μ2 phosphorylation stimulated binding by 5-fold (see Table 2 for rate constants), consistent with our earlier observations. However, when the TGN38-sorting signal was presented in membranes without PtdIns(4,5)P_2 (curves 3 and 4), no specific binding of AP2 cores to the signal was detectable, because the interaction was comparable to that observed for membranes containing PtdIns(4,5)P_2 only (curve 5). (B) When AP2 core mutants were injected, it became evident that disruption of the PtdIns(4,5)P_2 binding site in α-adaptin totally abolished AP2 binding (curves 3 and 4), whereas AP2 with a nonfunctional binding site for tyrosine signals in μ2 bound to the PtdIns4,5$_2$-Y surface (curve 1) with an affinity comparable to that observed for membranes containing only PtdIns(4,5)P_2. (C) The injection of C-μ2 and the C-μ2^{PIP-} mutant over the same surfaces demonstrated that C-μ2 on its own can recognize the TGN38 sorting signals irrespective of the membrane composition; however, PtdIns(4,5)P_2 stabilizes C-μ2 binding (compare curves 1 and 2).

(D) Depletion of PtdIns(4,5)P_2 inhibits the association of the EGFR with AP2. COS7 cells overexpressing either the EGFR alone or in combination with the membrane-targeted 5′-phosphatase domain of synaptojanin 1 (HA-IPP-CAAX) were lysed and subjected to immunoprecipitations by using antibodies against AP2 α-adaptin or a control protein (GAD). Nontransfected COS7 cells were assayed as further control. Aliquots of each supernatant (30 μg of total protein corresponding to 10% of total input) and of bound material obtained after extensive washing were analyzed on separate SDS gels followed by immunoblotting for α-adaptin A, EGFR, or tubulin. About 70% of the total AP-2 present in the lysates could be immunoprecipitated.

nonoverlapping with the Yxxϕ binding site. The apparent discrepancy with recently published work (Janvier et al., 2003) may be due to poor solubility of the material (α/σ2 heterodimer) used in that study. Our data also show that AP2 phosphorylation at μ2-Thr156 specifically modulates binding of Yxxϕ signals only, indicating that a conformational change is not required to allow binding of dileucine motifs.

Although binding of the phosphorylated CD4 dileucine motif (the strongest dileucine signal) was significantly weaker (~900 nM) than that recorded for the Yxxϕ signal of TGN38 (the strongest Yxxϕ signal, ~70 nM), it was still specific, because preincubation of AP2 with the soluble CD4 peptide (or other dileucine signal-containing peptides) abrogated binding to the membrane-attached CD4 tail peptide but did not affect recognition of Yxxϕ signals. In contrast, when AP2 was preincubated with a soluble TGN38 peptide, binding to the CD4 tail peptide was unaffected (data not shown). However, as with the binding of Yxxϕ motifs to AP2, the binding of dileucine signals to AP2 displayed in a membrane is also dependent on the presence of PtdIns4,5P_2 in that membrane. As seen for Yxxϕ motifs, mutant α^{PIP-} P-Core did not bind to PtdIns4,5P_2/dileucine-containing membranes above background levels (Figure 5C) . This presumably reflects that in both cases the initial recruitment of AP2 requires the interaction of PtdIns4,5P_2 with its binding site on the α subunit.

In order to further confirm that acidic dileucine motifs can interact with AP2 in living cells, the in vivo uptake of a chimeric molecule consisting of the extracellular portion of CD8 fused to the cytoplasmic tail of CD3 that

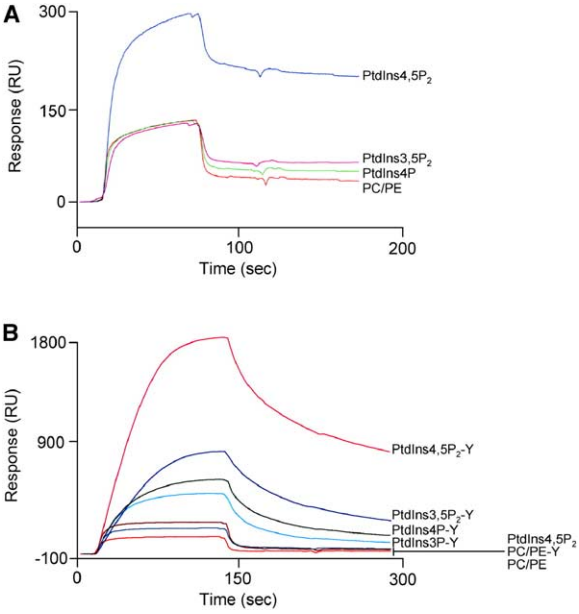

Figure 4. Binding of AP2 to TGN38 in Combination with Different Phosphoinositides

(A) Binding of AP2 to membranes was recorded as described in Figure 3. In order to monitor the influence of the various phosphoinositides on TGN38 binding, liposomes containing PC/PE and the TGN38 Yxxϕ motif were supplemented with 10% of one of the indicated phosphoinositides. Liposomes containing PC/PE only, PC/PE + PtdIns4,5P_2, and PC/PE + Yxxϕ motif served as controls. Because only four membranes can be probed simultaneously, PC/PE and PC/PE + PtdIns4,5P_2-Y were always used as a reference, and only the other two flow cells were coated with membranes of varying composition. The curves presented are therefore derived from several experiments performed sequentially.

(B) Binding of P-Core to PC/PE membranes and those containing signal but no phosphoinositide was negligible. Significant binding of AP2 could be recorded when the tyrosine motif was presented together with a phosphoinositide. Presence of PtdIns4,5P_2 resulted in the highest affinity of P-Core (K_D = 72 nM) but was much weaker and more transient when PtdIns4,5P_2 was substituted by one of the other phosphoinositides (PtdIns3P K_D = 680 nM, PtdIns4P K_D = 650 nM, and PtdIns3,5P_2 K_D = 550 nM).

contains a nonphosphorylatable dileucine internalization signal within its cytoplasmic tail was studied in cells that had been rendered AP2 or clathrin deficient by RNA interference (by using RNAi oligonucleotides as in Motley et al. [2003], depletion of both AP2 and clathrin heavy chain was greater than 90% as judged by Western blot analysis; data not shown). In cells depleted of AP2 or clathrin, the chimera remained on the cell surface, whereas in cells in which AP2 levels were normal, the CD8/dileucine chimera was rapidly internalized into the endocytic vesicles (Figure 5D). These data show that dileucine motif-containing cargo is endocytosed from the cell surface in an AP2- and clathrin-dependent manner.

Discussion

By using a number of techniques, including a new membrane mimic SPR binding assay and recombinant phosphorylated or unphosphosphorylated AP2 cores (both native and forms containing structure-directed mutations in key functional residues), we have shown that binding to endocytic motif-containing cargo is intimately coupled to the binding of phosphoinositides. When both cargo and the correct PIP, i.e., PtdIns4,5P_2 in the case of AP2, are present in a phospholipid membrane, these are necessary and sufficient to result in recruitment and tight binding of μ2 Thr156-phosphorylated AP2. These data help to explain the exclusive localization of AP2 to the cell's limiting membrane and not to internal organellar membranes where protein cargo is displayed in an incorrect or "nonpermissive" PIP context such as PtdIns3P/PtdIns3,5P_2 on the endosomal system or PtdIns4P on the TGN. In addition, in the in vivo situation, preferential association of AP2 with transmembrane cargo presented within PtdIns4,5P_2-containing membranes will be accentuated by the fact that other AP2 binding proteins known to bind to PtdIns4,5P_2 are concentrated at the plasma membrane. These include the amphiphysins, epsins and AP180/CALM, β-arrestins, Dab2, and ARH (which bind to the AP2 appendages; reviewed in Owen et al. [2004]) as well as synaptotagmin (which binds to the μ2 subunit, Grass et al., 2004). We thus propose that cargo recognition by AP adaptors is governed by the phosphoinositide environment in which the cargo is embedded, i.e., instructions defining transport for a cargo must be read in the context of a phosphoinositide code. However, these data do not rule out the possibility that other "docking factors" for AP2, for example a plasma membrane resident protein or a small GTPase, could assist PtdIns4,5P_2 in targeting AP2 to the plasma membrane.

Our data support a two-step model for productive binding of AP2 to the plasma membrane. The initial binding of AP2 to membranes is likely to be mediated via a relatively weak interaction of PtdIns4,5P_2 with a site on the α subunit (apparent K_D = 5–10 μM), which may also include a minor contribution from the μ2 PtdIns4,5P_2 binding site. This initial docking interaction of AP2 with the plasma membrane would be dynamic and readily reversible. In order to bind to Yxxϕ-containing cargo, a conformational change from the closed form is required that is more energetically favorable in the μ2Thr156-phosphorylated form. This change will presumably involve the displacement of C-μ2 from its spatially compatible binding site on the rest of the AP2 core, thus allowing it to sample the local membrane environment. In this "conformation," AP2 would be able to simultaneously use its Yxxϕ motif and secondary PtdIns4,5P_2 binding sites on C-μ2 for attachment to the membrane. The simultaneous use of three membrane attachment sites on a single AP2 will strengthen the interaction of AP2 with the membrane, resulting in an effective overall K_D in the range of 50–100 nM. This long-lived, stable interaction of AP2 with both protein cargo and membrane phospholipids would now be able to trigger the assembly of cargo-containing, clathrin-coated pits and may serve as an important factor in facilitating CCV formation (Ehrlich et al., 2004). The binding of AP2 to membranes containing dileucine signals only is weaker (effective K_D less than 1 μM) than to membranes containing Yxxϕ signals only and is not enhanced by phosphorylation-induced conformational

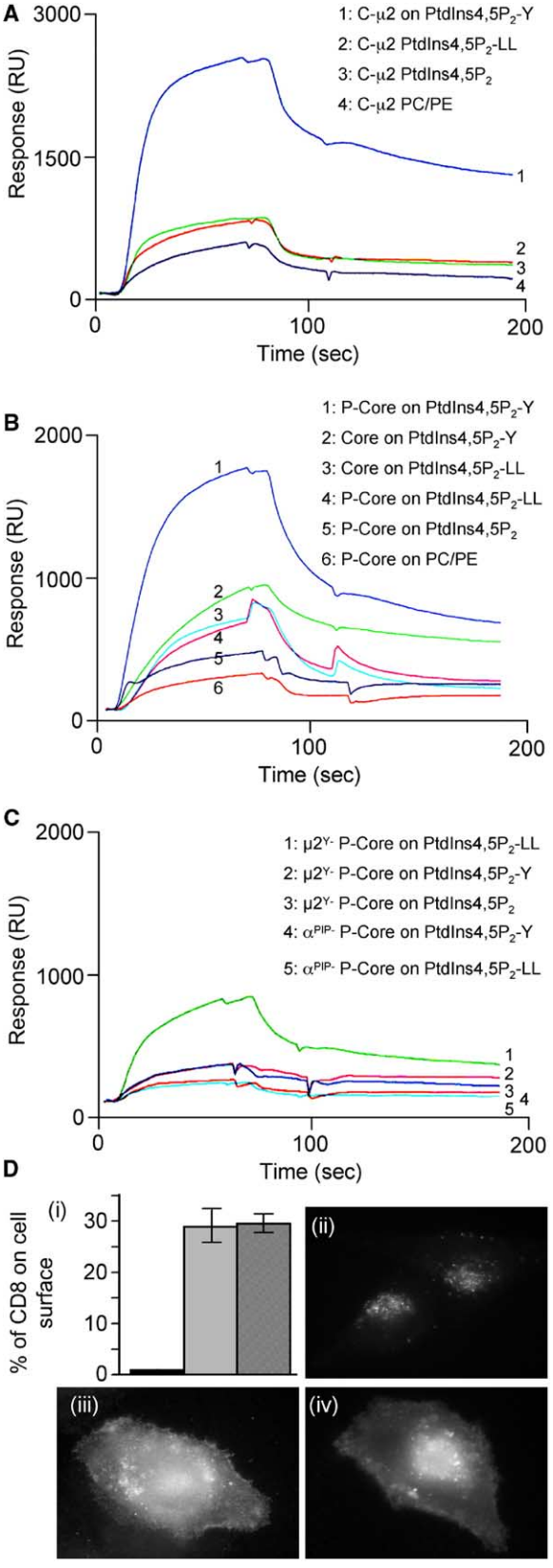

Figure 5. Binding of AP2 to Dileucine Signals

The L1 sensorchip was derivatized with control membranes (PC/PE), membranes containing PtdIns(4,5)P_2, membranes containing the tyrosine signal of TGN38 and PtdIns(4,5)P_2 (PtdIns4,5$_2$-Y), and membranes containing PtdIns(4,5)P_2 with the phosphorylated CD4 tail that harbors a dileucine signal (PtdIns4,5$_2$-LL).

(A) Recombinant C-μ2 bound with low-affinity binding to PtdIns(4,5)P_2 only (curve 4) and high-affinity binding to TGN38 in the presence of PtdIns(4,5)P_2 (curve 1) but showed no specific binding to CD4 in the presence of PtdIns(4,5)P_2 (curve 3).

(B) Binding of Core and P-Core to the TGN-sorting signal as described above (curves 1 and 2) also detected weak but significant binding to the dileucine signal, which was not affected by μ2 phosphorylation (compare curves 3 and 4).

(C) Mutation of the PtdIns(4,5)P_2 binding site in α-adaptin not only abolished binding to TGN38 but also to the dileucine signal of CD4 (curves 4 and 5). In contrast, mutation of the tyrosine binding site in μ2 abolished AP2 binding to TGN38 (curve 2) but did not affect binding to CD4 (curve 1).

(D) HeLaM cells stably expressing a CD8 construct with the tail sequence RRQRKSRRTIDKQTLL were depleted of either AP2 or clathrin heavy chain by using siRNAs (see Motley et al., 2003). (i) The binding of anti-CD8 to the cell surface was quantified by using ^{125}I-protein A (see Experimental Procedures). The bar graphs show the mean binding of anti-CD8 antibody to the cell surface (normalized to 1 for the control) ± the SD – control (black), AP2 depletion (gray), and clathrin depletion (hashed). (ii–iv) The steady-state distribution of the CD8 construct was determined by immunofluorescence – (ii) control (no depletion), (iii) AP2 depletion, (iv) and clathrin depletion.

change (effective K_D for phosphorylated AP2 binding to Yxxϕ motif containing membranes is less than 100 nM). This is presumably, in part, because there need not be binding to the μ2 PtdIns4,5P_2 binding site, which can only occur after C-μ2 displacement, in order for binding of the whole complex to a membrane-embedded dileucine motif-containing cargo. Moreover, association of dileucine motifs with their cognate recognition site within AP2 appears to be inherently weaker than binding to Yxxϕ motifs (as demonstrated by binding of AP2 cores to different motifs immobilized on carboxymethylated dextran sensor chips; data not shown). The in vivo situation may be more complex than the model presented here, as the plasma membrane contains both types of AP2 binding endocytic cargo proteins. It is thus possible that recognition of dileucine motifs benefits from the additional presence of Yxxϕ motif cargo, which may help to stabilize AP2 at the membrane, thereby indirectly increasing internalization rates.

The exact location of the dileucine motif binding site within AP2 cannot be determined from this work, although we have shown that it is not on C-μ2. Furthermore, it must be accessible in the absence of a μ2-phosphorylation-induced conformational change within AP2. It seems possible that the two states of AP2 defined here, a relatively weakly bound state dependent on the α trunk PtdIns4,5P_2 binding site and a tightly bound state employing both PtdIns4,5P_2 binding sites as well as Yxxϕ cargo motif association, may correspond to readily dissociable and the productively bound AP2 fractions seen recently in high-resolution live cell imaging studies (Ehrlich et al., 2004). CCV formation at long-lived, cargo-containing AP2 nucleation sites is expected to be further modulated by crosslinking of individual AP2 molecules by the multivalent clathrin scaffold and its accessory proteins. Such additional cooperative interactions would enhance the strength

of binding between the membrane and the now effectively polymerized AP2s, further increasing the lifetime of the coat beyond that of a single AP2 molecule. It may well be possible to extend this SPR-based assay to study assembly and disassembly of adaptor/clathrin coats by adding clathrin itself as well as regulatory molecules (e.g., phosphatases) simultaneously or sequentially with the soluble adaptors. The membrane mimic recruitment assay presented here in which liposomal membranes of defined phospholipid and protein/peptide content are used to accurately measure and dissect the mechanism of the recruitment of soluble proteins could further be used to answer questions concerning the formation of other cargo-selective coats by altering the lipid, cargo, and peripheral proteins used.

Experimental Procedures

Production of Phosphorylated AP2 Cores

Coexpression of recombinant AP2 cores in *E. coli* was as described in Collins et al. (2002). In order to make phosphorylated AP2 cores, an untagged fragment containing residues 1–325 (the catalytic domain) of rat AAK1 preceded by a translational control region was cloned into the pMWH6β2μ2 vector after the μ2 gene. Expression and purification was carried out as for production of nonphosphorylated complex. Mutations were introduced into Core and P-Core by megaprimer PCR mutagenesis, and expression and purification of these constructs was as for wt complexes.

Nanoelectrospray Mass Spectrometry

Mass spectra were acquired on a LCT (Micromass, UK) and on a tandem mass spectrometer Q-TOF 2 (Micromass, UK) modified for high mass operation and equipped with a Z spray nanoflow electrospray interface (see Supplemental Data). Dissociation and proteolytic digestion of samples were as described in the Supplemental Data.

Peptides Sequences and Conjugation of Peptides to Lipid

Sorting signal-containing peptides derived from the cytoplasmic tails of TGN 38 (CKVTRRPKASDYQRL) and phosphorylated CD4 (CHRRRQAERM[S*]QIKRLLSEK) (the asterisk indicates the phosphorylated residue) were synthesized with an amino-terminal cysteine. The quality of all peptides was controlled by mass spectrometry after reverse-phase chromatography. For covalent conjugation of a peptide to a synthetic lipid, 5 mmol peptide in 1 ml 10 mM MOPS-KOH (pH 7.5), 50% DMF were mixed with an equal volume lipid (1,2-dipalmitoyl-sn-glycero-3-phosphoethanolamine-N-[4-(p-maleimidophenyl)butyramide], Avanti, USA) at 5 mg/ml in chloroform and incubated for 2 hr at 20°C under end-over-end rotation. Coupling was blocked by addition of β-mercaptoethanol to a final concentration of 10 mM and further incubation for 30 min. The lipid-linked peptide was collected from the organic phase after extraction with 2 ml chloroform and 1 ml methanol and dried under nitrogen. The dried peptido-lipid was resuspended in chloroform/methanol (2:1) at 5 mg/ml and stored at –20°C.

Synthesis of Liposomes

All lipids (phosphatidylcholine, phosphatidylethanolamine, and the phosphoinositides PtdIns3P, PtdIns4P, PtdIns4,5P_2, and PtdIns3,4,5P_3) were stored in chloroform/methanol in a nitrogen atmosphere. For preparation of basic liposomes (80% PC, 20% PE), the appropriate amounts (w/w) were mixed and dried under nitrogen and rehydrated with 150 μl of 0.3 M sucrose for 1 hr before the volume was adjusted to 1 ml by using H_2O. The liposomes were then sedimented by centrifugation at 20,000 rpm for 1 hr at 4°C (TLA 120 rotor, Beckman tabletop) and resuspended in 500 μl 20 mM HEPES, (pH 7.4). To prepare unilamellar liposomes, the liposome solution was passed 15 times through an extruder by using a 100 nm membrane (LiposoFast, Avestin, Canada) and kept for further use at 4°C. Complex liposomes were prepared by substitution of 10% PC by the equivalent amount of lipid-linked peptide and/or one of the mentioned phosphoinositides.

Liposome Pulldowns

Purified AP2 cores were diluted (40 μg/ml final concentration) into cytosolic buffer (25 mM HEPES-KOH [pH 7.2], 25 mM KCl, 150 mM K-glutamate, and 2.5 mM magnesium acetate) and precleared by ultracentrifugation for 30 min at 150,000 × g. Samples were mixed with 100 μg freshly prepared liposomes (1 mg/ml final lipid concentration) and incubated for 5 min at 20°C. Binding reactions were chilled on ice, and liposomes were reisolated by ultracentrifugation, washed, and analyzed by SDS-PAGE and staining with Coomassie blue or immunoblotting developed with ^{125}I-protein A.

Biosensor Experiments

For methods concerning pilot experiments using synthetic tail peptides immobilized on CM5 surfaces, see the Supplemental Data.

Lipososmes and peptido-liposomes were used to generate a stable membrane mimic on a special sensor surface (L1) of a SPR-based biosensor (BIAcore 3000, BIAcore AB, Sweden) to subsequently record binding of AP2 cores and C-μ2 in real time. The L1 sensor surface consisted of a carboxy-methyl dextran hydrogel derivatised with lipophilic alkyl chains that allowed capture of injected liposomes. The L1 surface was primed with an injection of 20 mM CHAPS for 1 min at a flow rate of 10 μl/min. Subsequently, the liposomes (diluted 1:5 in running buffer) were injected at 5 μl/min for 15 min followed by pulse injections of 50 mM sodium hydroxide and 100 mM hydrochloric acid at 20 μl/min to remove unbound material. This procedure resulted in an increase of the baseline by 9000–10,500 RU that remained stable for more than 30 experimental cycles. Electron microscopy of cross-sections derived from a liposome-derivatized L1 surface demonstrated the stability and integrity of the immobilized liposomes (the exact methodology is available upon request). All binding experiments with μ2 were performed in 10 mM HEPES (pH 7.4), 500 mM NaCl, whereas 10 mM Tris (pH 8.7), 250 mM NaCl was used as a running buffer in experiments with AP2 complexes. μ2 and AP2 were used at concentrations ranging from 200 nM to 5 μM at a flow rate of 10 μl/min. All protein that did not dissociate within 5 min from the membrane mimic surface was stripped off by a pulse injection of 50 mM NaOH. Removal of captured lipid from the L1 sensor surface was performed in a regeneration process at a flow rate of 5 μl/min by injections of 0.5% SDS, H_2O, 1% TX-100, H_2O, 30% 2-Propanol, and H_2O (each injection for 5 min). All rate constants were calculated by using the Evaluation software supplied by the manufacturer. Details about the calculation are described in the Supplemental Data.

Coimmunoprecipitation Experiments

Cos7 cells were transfected with plasmids encoding the EGFR (HERc/pRK5; a kind gift from Dr. Axel Ullrich, Max-Planck Institute, Martinsried) and/or HA-CAAX-IPPase by using Lipofectamine 2000. 2 days posttransfection, cells were lysed in TGH buffer (1% TX100, 10% glycerol, 50 mM NaCl, 50 mM HEPES [pH 7.5], 1 mM EGTA, and 1% Na-deoxycholate), precleared by ultracentrifugation, and subjected to immunoprecipitation with antibodies against AP2α (AP.6) or γ-glutamic acid decarboxylase 67 (GAD67; as a control) immobilized on protein G sepharose. Nonbound material was precipitated with TCA/aceton. Bead bound samples were washed extensively and eluted with sample buffer. Aliquots of bound (from cell lysates containing 300 μg protein) and nonbound material (30 μg of total protein) were analyzed by SDS-PAGE and immunoblotting.

Internalization Experiments

A CD8 chimera with a dileucine-containing tail was constructed in pIRES by using a double-stranded oligonucleotide, as described by Seaman (2004). The sequence of the tail, RRQRKSRRTIDKQTLL, is derived from CD3γ. HeLa M cells stably transfected with this construct were depleted of either μ2 or clathrin heavy chain by using siRNAs, as previously described (Motley et al., 2003). Immunofluorescence was carried out as previously described (Motley et al., 2003), using a monoclonal antibody against CD8 (153-020, An-

cell Corp.). This antibody was also used to quantify the amount of chimera on the cell surface. Cells were incubated in serum-free medium with a 1:100 dilution of the antibody for 45 min at 4°C, then washed and incubated for a further 45 min at 4°C in serum-free medium containing a 1:1000 dilution of ^{125}I-protein A (Amersham). The cells were solubilized with 1 M NaOH, and radioactivity was quantified using a γ counter (Nuclear Enterprises). Results shown are the average of three independent experiments.

Supplemental Data

Supplemental Data include Supplemental Experimental Procedures, Supplemental References, two figures, and two tables and are available with this article online at http://www.molecule.org/cgi/content/full/18/5/519/DC1/.

Acknowledgments

We thank Dr. A. Ullrich (Max-Planck Institute for Biochemistry, Martinsried, Germany) for the kind gift of the EGFR-encoding plasmid and Brett Collins and Phil Evans for their help and critically reading the manuscript. This work was supported by grants from the Deutsche Forschungsgemeinschaft (SFB 523, TPA5) to S.H. and V.H. (TP B8 and SFB 366 TP B11) and a Wellcome Trust Senior Fellowship in Basic Biomedical Sciences to D.J.O. V.H. and D.J.O. are EMBO Young Investigators.

Received: February 17, 2005
Revised: April 14, 2005
Accepted: April 27, 2005
Published: May 26, 2005

References

Bonifacino, J.S., and Traub, L.M. (2003). Signals for sorting of transmembrane proteins to endosomes and lysosomes. Annu. Rev. Biochem. *72*, 395–447.

Collins, B.M., McCoy, A.J., Kent, H.M., Evans, P.R., and Owen, D.J. (2002). Molecular architecture and functional model of the endocytic AP2 complex. Cell *109*, 523–535.

Conner, S.D., and Schmid, S.L. (2002). Identification of an adaptor-associated kinase, AAK1, as a regulator of clathrin-mediated endocytosis. J. Cell Biol. *156*, 921–929.

Cooper, M.A., Hansson, A., Lofas, S., and Williams, D.H. (2000). A vesicle capture sensor chip for kinetic analysis of interactions with membrane-bound receptors. Anal. Biochem. *277*, 196–205.

De Matteis, M.A., and Godi, A. (2004). PI-loting membrane traffic. Nat. Cell Biol. *6*, 487–492.

Ehrlich, M., Boll, W., Van Oijen, A., Hariharan, R., Chandran, K., Nibert, M.L., and Kirchhausen, T. (2004). Endocytosis by random initiation and stabilization of clathrin-coated pits. Cell *118*, 591–605.

Gaidarov, I., Chen, Q., Falck, J.R., Reddy, K.K., and Keen, J.H. (1996). A functional phosphatidylinositol 3,4,5-trisphosphate/phosphoinositide binding domain in the clathrin adaptor AP-2 alpha subunit. Implications for the endocytic pathway. J. Biol. Chem. *271*, 20922–20929.

Ghosh, P., and Kornfeld, S. (2003). AP-1 binding to sorting signals and release from clathrin-coated vesicles is regulated by phosphorylation. J. Cell Biol. *160*, 699–708.

Grass, I., Thiel, S., Höning, S., and Haucke, V. (2004). Recognition of a basic AP-2 binding motif within the C2B domain of synaptotagmin is dependent on multimerization. J. Biol. Chem. *279*, 54872–54880.

Heldwein, E.E., Macia, E., Wang, J., Yin, H.L., Kirchhausen, T., and Harrison, S.C. (2004). Crystal structure of the clathrin adaptor protein 1 core. Proc. Natl. Acad. Sci. USA *101*, 14108–14113.

Hicke, L., and Dunn, R. (2003). Regulation of membrane protein transport by ubiquitin and ubiquitin-binding proteins. Annu. Rev. Cell Dev. Biol. *19*, 141–172.

Huang, F., Khvorova, A., Marshall, W., and Sorkin, A. (2004). Analysis of clathrin-mediated endocytosis of epidermal growth factor receptor by RNA interference. J. Biol. Chem. *279*, 16657–16661.

Jackson, A.P., Flett, A., Smythe, C., Hufton, L., Wettey, F.R., and Smythe, E. (2003). Clathrin promotes incorporation of cargo into coated pits by activation of the AP2 adaptor micro2 kinase. J. Cell Biol. *163*, 231–236.

Janvier, K., Kato, Y., Boehm, M., Rose, J.R., Martina, J.A., Kim, B.Y., Venkatesan, S., and Bonifacino, J.S. (2003). Recognition of dileucine-based sorting signals from HIV-1 Nef and LIMP-II by the AP-1 gamma-sigma1 and AP-3 delta-sigma3 hemicomplexes. J. Cell Biol. *163*, 1281–1290.

Krauss, M., Kinuta, M., Wenk, M.R., De Camilli, P., Takei, K., and Haucke, V. (2003). ARF6 stimulates clathrin/AP-2 recruitment to synaptic membranes by activating phosphatidylinositol phosphate kinase type Igamma. J. Cell Biol. *162*, 113–124.

Motley, A., Bright, N.A., Seaman, M.N., and Robinson, M.S. (2003). Clathrin-mediated endocytosis in AP-2-depleted cells. J. Cell Biol. *162*, 909–918.

Nesterov, A., Carter, R.E., Sorkina, T., Gill, G.N., and Sorkin, A. (1999). Inhibition of the receptor-binding function of clathrin adaptor protein AP-2 by dominant-negative mutant mu2 subunit and its effects on endocytosis. EMBO J. *18*, 2489–2499.

Ohno, H., Stewart, J., Fournier, M.C., Bosshart, H., Rhee, I., Miyatake, S., Saito, T., Gallusser, A., Kirchhausen, T., and Bonifacino, J.S. (1995). Interaction of tyrosine-based sorting signals with clathrin-associated proteins. Science *269*, 1872–1875.

Olusanya, O., Andrews, P.D., Swedlow, J.R., and Smythe, E. (2001). Phosphorylation of threonine 156 of the mu2 subunit of the AP2 complex is essential for endocytosis in vitro and in vivo. Curr. Biol. *11*, 896–900.

Owen, D.J., and Evans, P.R. (1998). A structural explanation for the recognition of tyrosine-based endocytotic signals. Science *282*, 1327–1332.

Owen, D.J., Collins, B.M., and Evans, P.R. (2004). Adaptors for clathrin coats: structure and function. Annu. Rev. Cell Dev. Biol. *20*, 153–191.

Padron, D., Wang, Y.J., Yamamoto, M., Yin, H., and Roth, M.G. (2003). Phosphatidylinositol phosphate 5-kinase Ibeta recruits AP-2 to the plasma membrane and regulates rates of constitutive endocytosis. J. Cell Biol. *162*, 693–701.

Pauloin, A., and Thurieau, C. (1993). The 50 kDa protein subunit of assembly polypeptide (AP) AP-2 adaptor from clathrin-coated vesicles is phosphorylated on threonine-156 by AP-1 and a soluble AP50 kinase which co-purifies with the assembly polypeptides. Biochem. J. *296*, 409–415.

Pitcher, C., Honing, S., Fingerhut, A., Bowers, K., and Marsh, M. (1999). Cluster of differentiation antigen 4 (CD4) endocytosis and adaptor complex binding require activation of the CD4 endocytosis signal by serine phosphorylation. Mol. Biol. Cell *10*, 677–691.

Praefcke, G.J., Ford, M.G., Schmid, E.M., Olesen, L.E., Gallop, J.L., Peak-Chew, S.Y., Vallis, Y., Babu, M.M., Mills, I.G., and McMahon, H.T. (2004). Evolving nature of the AP2 alpha-appendage hub during clathrin-coated vesicle endocytosis. EMBO J. *23*, 4371–4383.

Rapoport, I., Chen, Y.C., Cupers, P., Shoelson, S.E., and Kirchhausen, T. (1998). Dileucine-based sorting signals bind to the beta chain of AP-1 at a site distinct and regulated differently from the tyrosine-based motif-binding site. EMBO J. *17*, 2148–2155.

Ricotta, D., Conner, S.D., Schmid, S.L., von Figura, K., and Höning, S. (2002). Phosphorylation of the AP2 mu subunit by AAK1 mediates high affinity binding to membrane protein sorting signals. J. Cell Biol. *156*, 791–795.

Robinson, M. (1993). Assembly and targeting of adaptin chimeras in transfected cells. J. Cell Biol. *123*, 67–77.

Rodionov, D.G., and Bakke, O. (1998). Medium chains of adaptor complexes AP-1 and AP-2 recognize leucine-based sorting signals from the invariant chain. J. Biol. Chem. *273*, 6005–6008.

Rohde, G., Wenzel, D., and Haucke, V. (2002). A phosphatidylinosi-

tol (4,5)-bisphosphate binding site within mu2-adaptin regulates clathrin-mediated endocytosis. J. Cell Biol. *158*, 209–214.

Seaman, M.N. (2004). Cargo-selective endosomal sorting for retrieval to the Golgi requires retromer. J. Cell Biol. *165*, 111–122.

Sorkin, A., Mazzotti, M., Sorkina, T., Scotto, L., and Beguinot, L. (1996). Epidermal growth factor receptor interaction with clathrin adaptors is mediated by the Tyr974-containing internalization motif. J. Biol. Chem. *271*, 13377–13384.

Traub, L.M. (2003). Sorting it out: AP-2 and alternate clathrin adaptors in endocytic cargo selection. J. Cell Biol. *163*, 203–208.

Umeda, A., Meyerholz, A., and Ungewickell, E. (2000). Identification of the universal cofactor (auxilin 2) in clathrin coat dissociation. Eur. J. Cell Biol. *79*, 336–342.

Wang, Y.J., Wang, J., Sun, H.Q., Martinez, M., Sun, Y.X., Macia, E., Kirchhausen, T., Albanesi, J.P., Roth, M.G., and Yin, H.L. (2003). Phosphatidylinositol 4 phosphate regulates targeting of clathrin adaptor AP-1 complexes to the Golgi. Cell *114*, 299–310.

Supplemental Data

Phosphatidylinositol-(4,5)-Bisphosphate Regulates Sorting Signal Recognition by the Cathrin-Associated Adaptor Complex AP2

Stefan Höning, Doris Ricotta, Michael Krauss, Kira Späte, Barbara Spolaore, Alison Motley, Margaret Robinson, Carol Robinson, Volker Haucke, and David Owen

Supplemental Experimental Procedures

Mass spectrometry materials and methods

Sample preparation and tryptic digestion of the phosphorylated and non-phosphorylated AP2 complex for mass spectrometry.

AP2 samples were stored at 4°C and buffer-exchanged twice with 200 mM ammonium acetate, pH 7.5 using microcentrifuge columns (Micro Bio-spin 6, Bio-Rad) before analysis. Buffer exchange and sample introduction were conducted at room temperature. Dissociation of the complex was performed by treating the sample in 200 mM ammonium acetate at pH 7.5 with a cation exchange matrix (AG 50W-X8 matrix, Bio-Rad). This treatment effectively reduces the pH to between 2 and 3 and this causes the subunits to dissociate. Tryptic digestion was performed on samples of phosphorylated and non-phosphorylated AP2 buffer exchanged to 200 mM ammonium acetate, pH 7.5 and at a complex concentration of 1.5-2.0 mg/ml, estimated by measuring the absorbance at 280 nm. Proteolysis was initiated by adding a stock solution of bovine pancreatic tryspin at a protein/enzyme ratio of 1/50 by weight. The digestions were performed at 37°C in a thermostated bath and stopped after 1 hour by dilution of aliquots of the reaction mixture 2-fold with a solution of 3% acetic acid in acetonitrile.

Nano-electrospray mass spectrometry.

Mass spectra were acquired on a LCT (Micromass, UK) and on a tandem mass spectrometer Q-TOF 2 (Micromass, UK) modified for high mass operation (Sobott et al 2002) and equipped with a Z-spray nanoflow electrospray interface. Nano-ESI capillaries were prepared in house from borosilicate glass tubes of 1 mm OD and 0.78 mm ID (Harvard Apparatus, Holliston, MA, USA) using a Flaming/Brown P-97 micropipette puller (Sutter Instruments, Hercules, CA, USA), and gold coated using a SEM sputter coater (Polaron, Newhaven, UK). The capillary tips were cut under a stereomicroscope to give inner diameters of 1-5 μm, and typically 0.5-2 μl of solution were loaded for sampling. For the analysis of the intact AP2 complex, pressures and accelerating voltages in the Q-TOF 2 mass spectrometer were adjusted to preserve non-covalent interactions. The following experimental parameters were typically used (positive ion mode): capillary voltage, 1.8 kV; sample cone, 200 V; extractor cone, 100 V; collision energy, 4 V; ion transfer stage pressure 3.2×10^{-3} mbar; quadrupole analyser pressure, 1.8×10^{-5} mbar; TOF analyser pressure, 4.7×10^{-7} mbar; and spectrum acquisition frequency, 3.9 kHz. Analysis of the tryptic digest and MS/MS experiments were performed under the same pressure conditions as above but using a capillary voltage of 1.5 kV, a sample cone of 80 V and an extractor cone set to 0 V. No heating was applied in the electrospray source. For MS/MS, the quadrupole resolution was set to transmit a mass window of ~1 Th for parent ion selection. The collision gas used was argon at an indicated inlet pressure of 30 psi and the collision energy setting was 35 V.

Spectra of the dissociated AP2 complex were acquired on the LCT (Micromass, UK) using a capillary voltage of 1.3 kV, a sample cone of 40 V and an extractor of 3 V, whereas pressure values were at base condition (1.89 mbar in the ion transfer stage pressure and 7.38 x 10^{-7} mbar as TOF analyser pressure). In both instruments external calibration was performed using a solution of cesium iodide. Instrument control and data acquisition and processing were achieved with MassLynx software (Micromass, UK). All spectra reported are shown with minimal smoothing and without background subtraction.

Mass spectrometry Results and Discussion

Analysis of the intact P-Core complex under conditions where non-covalent interactions are preserved indicated that only one charge state series is present centered at 7000 m/z, which corresponds to a mass of 206148.6Da (Supplementary Figure 1A). This is a difference only of the 0.08% from the theoretical mass of 205989.8Da. The measured masses for the low pH dissociated individual subunits (shown in Supplementary Figure1b) are close to the theoretical values for α, β2 and σ2, whereas for the μ2 subunit a mass of 51055.4 was measured, which corresponds to the theoretical mass of the mono-phosphorylated protein (51051.3 Da). The μ2 subunit seems almost completely phosphorylated since we did not observe the charge state series corresponding to the non phosphorylated protein.

MS/MS sequence analysis of tryptic digests of the P-Core and Core demonstrated that phosphorylation occurred in the tryptic peptide 146-162 (data not shown and Fig 1C in main text) and furthermore from studying the fragmentation patterns it was shown that there was only one site of phosphorylation corresponding to Thr156, which is the site of *in vivo* phosphorylation by AAK1 (see Supplementary Fig. 1C and 1D). Analysis of the signal intensities for the 146-162 tryptic peptide from P-Core and Core indicated that the efficiency of phosphorylation was greater than 95% (see supplementary material). This high level of efficiency of phosphorylation is further emphasized by the fact that the ionisation efficiency of phosphorylated peptides in the positive mode are lower than those of the non phosphorylated ones, especially in the presence of other peptides (Bevilaqua et al 2001 : McLachlin et al 2001 : Mann et al 2002). For this reason, measuring the yield of the phosphorylation on the basis of the relative intensity of the signals can be an underestimate (Lawrie et al 2001). Studies on peptide mixtures of known stoichiometry of phosphorylated and non phosphorylated species with a nanoelectrospray source reported that low pH in the positive mode are optimal conditions for the determination of the ratio between the modified and non modified peptides, especially for phosphothreonine containing peptides. However, even in this case an underestimation around 30 % has been detected (Carr et al 1996).

This high stoichiometry of μ2Thr156 phosphorylation was consistent in three independently purified preparations of wild type P-Core that we examined as well as in the phosphorylated mutant forms of the core used in these studies (data not shown). The observation that only the kinase domain of AAK1 is required to obtain virtually complete phosphorylation on only the desired (i.e *in vivo* site) indicates that sufficient peptide substrate specificity determinants required by AAK1 to phosphorylate the μ2 subunit of AP2 are contained within the kinase core, which is in line with structural studies on other kinases (Lowe et al 1997) and as predicted by the kinase substrate prediction programme (Brinkworth et al., 2003). *In vivo* additional substrate specificity for the kinase may come from the kinase's localisation in CCPs determined largely by its interaction with clathrin and the α-appendage of AP2 (Jackson et al., 2003; Conner et al., 2003).

Supplemental References

Sobott, F., Hernandez, H., McCammon, M.G., Tito, M.A. & Robinson, C.V. (2002) A tandem mass spectrometer for improved transmission and analysis of large macromolecular assemblies. *Anal. Chem. 74*, 1402-7.

Mann, M., Ong, S.E., Gronborg, M., Steen, H., Jensen, O.N. & Pandey, A. (2002) Analysis of protein phosphorylation using mass spectrometry: deciphering the phosphoproteome. *Trends Biotechnol. 20*, 261-8.
McLachlin, D.T. & Chait, B.T. (2001) Analysis of phosphorylated proteins and peptides by mass spectrometry. *Curr. Opin. Chem. Biol. 5*, 591-602.
Bevilaqua, L.R., Graham, M.E., Dunkley, P.R., von Nagy-Felsobuki, E.I. & Dickson, P.W. (2001) Phosphorylation of Ser(19) alters the conformation of tyrosine hydroxylase to increase the rate of phosphorylation of Ser(40). *J. Biol. Chem. 276*, 40411-6.
Lawrie, A.M., Tito, P., Hernandez, H., Brown, N.R., Robinson, C.V., Endicott, J.A., Noble, M.E., Johnson, L.N. (2001) Xenopus phospho-CDK7/cyclin H expressed in baculoviral-infected insect cells. *Protein Expr. Purif. 23(2)*, 252-260.
Carr, S.A., Huddleston, M.J. & Annan, R.S. (1996) Selective detection and sequencing of phosphopeptides at the femtomole level by mass spectrometry. *Anal. Biochem. 239*, 180-92.
Lowe, E.D., Noble, M.E., Skamnaki, V.T., Oikonomakos, N.G., Owen, D.J. and Johnson, L.N. (1997). The crystal structure of a phosphorylase kinase peptide substrate complex: kinase substrate recognition. *Embo J*, **16**, 6646-6658.
Brinkworth, R.I., Breinl, R.A. and Kobe, B. (2003). Structural basis and prediction of substrate specificity in protein serine/threonine kinases. *Proc Natl Acad Sci U S A*, **100**, 74-79.

A

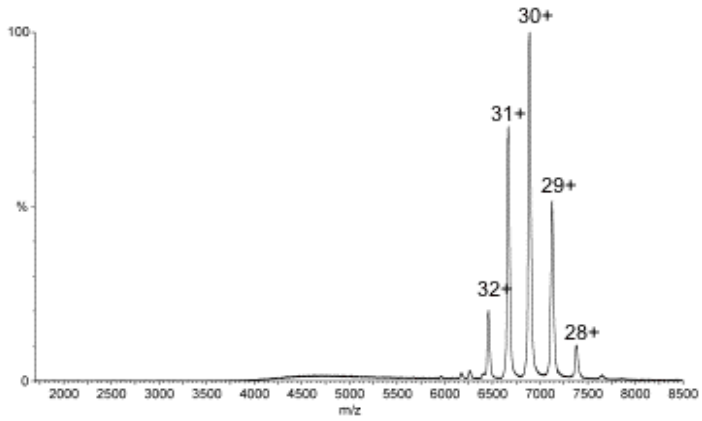

B

Protein	**Molecular mass (Daltons)**	
	Theoretical	Measured
α subunit	70092.2	70099.0+/-7.2
β2 subunit	67828.6	67840.0+/-3.1
μ2-P subunit	51051.3	51055.4+/-0.9
σ2 subunit	17017.8	17018.3=/-0.2

C

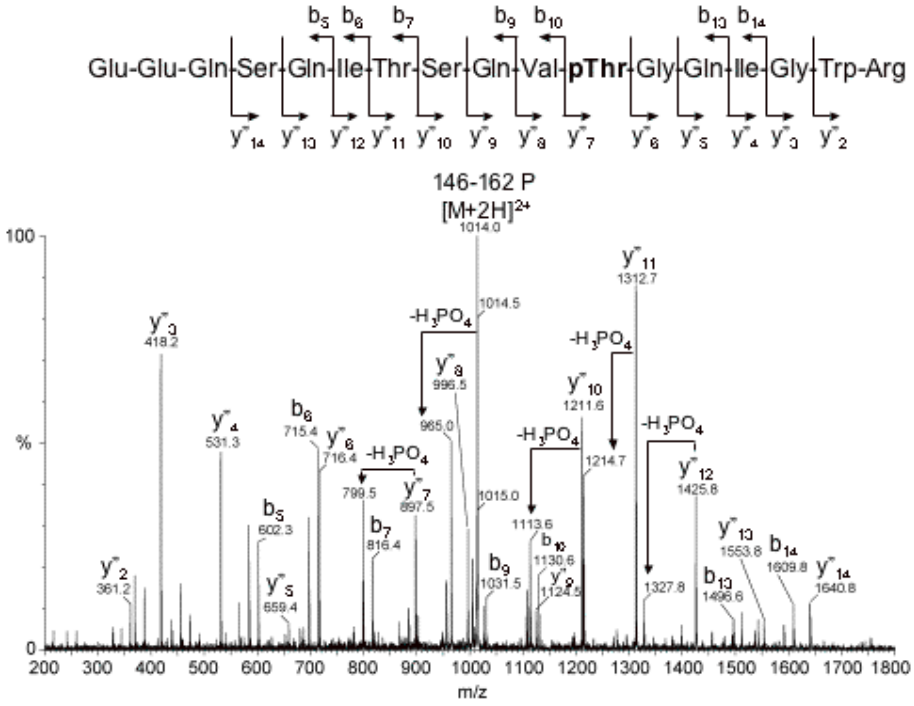

D

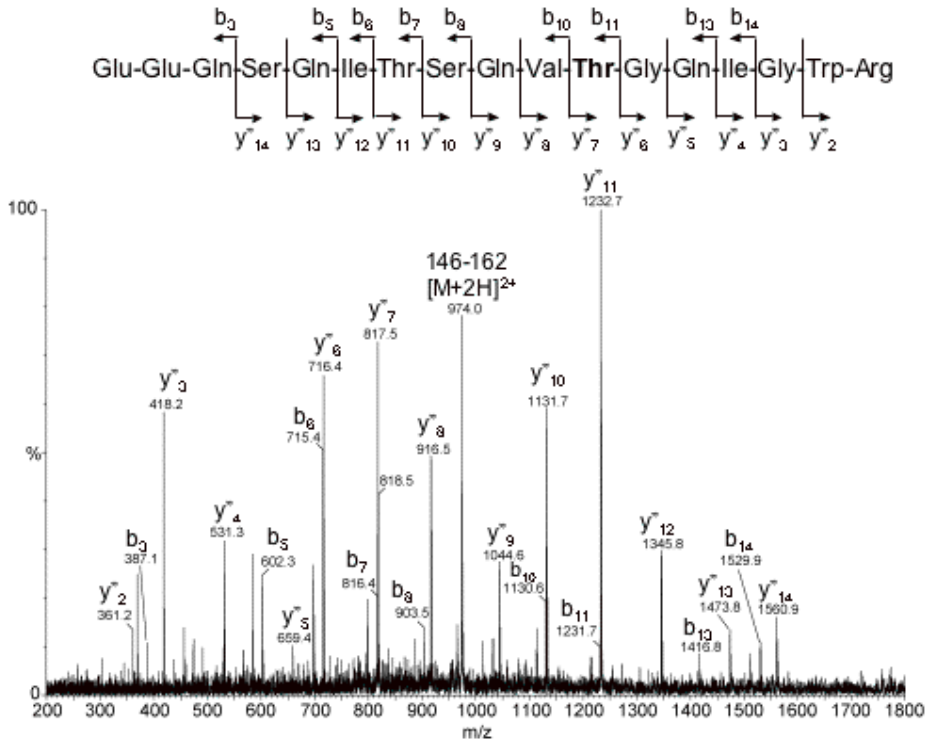

Figure S1

(A) Nano-electrospray mass spectra of the phosphorylated AP2 complex.
The intact complex analysed under conditions where non-covalent interactions are preserved. The charge state series of the complex is indicated. Only one charge state series is present centered at 7000 m/z, which corresponds to a mass of 206148.6Da.

(B) Predicted and measured molecular weights of phosphorylated AP2 core subunits

(C) and (D) Sequencing of μ2Thr156 phosphorylation site by analysis of MS/MS fragmentation pattern produced in the tryptic digest of the phosphorylated (C) and non-phosphorylated (D) AP2 cores. In the part of the fragmentation series which does not contain the potentially phosphorylated threonine the two samples show identical fragments, whereas the other part of the series containing Thr156 has a mass difference of 80 between the two spectra, which is the mass corresponding to the addition of a phosphate group. In both the MS/MS spectra the coverage of the sequence is quite high at ~ 70 %: 12 amino acids from 17. Only the identity of the isoleucine residues could not be confirmed due to the fact that isoleucine is isobaric with leucine. (C) MS/MS spectra of the phosphorylated peptide 146-162 $[M+2H]^{2+}$ ion. In the mass spectrum the y" and b ions and the loss of H_3PO_4 (-98Da) on fragmentation are indicated. The corresponding localisation of the product fragments in the sequence of the peptide 146-162 is also shown. (D) MS/MS spectra of the peptide 146-162 $[M+2H]^{2+}$ ion. In the mass spectrum the y" and b ions are indicated. The corresponding localisation of the product fragments in the sequence of the peptide 146-162 is also shown.

Surface Plasmon Resonance (Biosensor) Supplementary Information

Initial experiments to verify the functionality of recombinant AP2 cores (P-Core and Core) in comparison with the binding of recombinant C-μ2 and AP2 isolated from pig brain (as in Fingerhut et al., 2001) were made using the synthetic tail peptide of TGN38 (CKVTRRPKASDYQRL). The peptide was immobilized via the thiol group of its aminoterminal cysteine residue on a carboxy-methylated dextran (CM5) sensor surface using the thiol coupling strategy exactly following the manufactors instructions (BIAcore AB). After peptide immobilization (~1000RU) the surface was regenerated using pulse injections of 50mM NaOH and 50mM NaOH, 5% SDS to remove non-covalently bound peptide. The subsequent analysis of binding of purified AP2, recombinant AP2 cores or μ2 was carried out exactly as described (Ricotta et al., 2002) except that the running buffer used was 250mM NaCl, 10mMTris pH8.7 1mM DTT. The binding to a TGN38 peptide in which the critical tyrosine residue was substituted for alanine served as a control and was substracted before the rate constants were calculated using the Evaluation software supplied by the manufacturer (BIAcore evaluation software, Jonsson et al., 1991). The data obtained (shown in Supplementary Table 1) indicates that the recombinant proteins are at least as functional in their tyrosine-based signal bidning as AP2s isolated from intact porcine brain.

	AP2 (pig brain)			AP2 core			AP2 P-core			μ2 (157-435)		
	k_a ($M^{-1} \times s^{-1}$)	k_d (s^{-1})	K_D (nM)	k_a ($M^{-1} \times s^{-1}$)	k_d (s^{-1})	K_D (nM)	k_a ($M^{-1} \times s^{-1}$)	k_d (s^{-1})	K_D (nM)	k_a ($M^{-1} \times s^{-1}$)	k_d (s^{-1})	K_D (nM)
TGN38	5.1×10^3	2.6×10^{-3}	510	6.0×10^3	2.7×10^{-3}	450	8.2×10^4	2.9×10^{-3}	36	1.1×10^3	1.7×10^{-3}	1,500

Table S1. Rate constants for the binding of purified AP2, recombinant AP2 and μ2 to the sorting signal of TGN38. Analytes were passed over the peptide-derivatized surface for 2 min at 4 concentrations ranging from 100nM to 2μM. The rate constants were calculated from the obtained sensorgrams after substraction of binding to the mutant control peptide (see above).

The binding to other tail peptides listed below was also tested. As can be seen from Table S2 the various signals were bound with different affinities with the highest being that of TGN38 (450nM) (in line with data obtained from recombinant peptide library screening using recombinant C-μ2 (Ohno et al., 1998). The sequences of the sorting signal containing peptides used were derived from the cytoplasmic tails of
TGN 38 (CKVTRRPKASDYQRL)
Lamp-1 (CRKRSHAGYQTI)
LAP (CRMQAQPPGYRHV)
phosphorylated CD4 (CHRRRQAERM(S*P*)QIKRLLSEK)
Limp-II (CRGQGSTDEGTADERAPLIRT)
Tyrosinase (CKKQPQEERQPLLMDKDDYHSLLYQSHL)

	AP2 (pig brain)			AP2 core			AP2 core (phosphorylated)		
	K_a ($M^{-1} \times s^{-1}$)	K_d (s^{-1})	K_D (nM)	K_a ($M^{-1} \times s^{-1}$)	K_d (s^{-1})	K_D (nM)	K_a ($M^{-1} \times s^{-1}$)	K_d (s^{-1})	K_D (nM)
TGN38	5.1×10^3	2.6×10^{-3}	510	6.0×10^3	2.7×10^{-3}	450	8.2×10^4	2.9×10^{-3}	36
Lamp-1	3.3×10^3	2.5×10^{-3}	758	3.5×10^3	2.5×10^{-3}	714	5.1×10^4	2.7×10^{-3}	53
LAP	3.0×10^3	2.8×10^{-3}	933	3.3×10^3	2.8×10^{-3}	848	4.5×10^4	2.9×10^{-3}	64
Limp-II	1.5×10^3	3.5×10^{-3}	2,300	1.8×10^3	3.6×10^{-3}	2,000	2.0×10^3	3.8×10^{-3}	1,900
Tyrosinase	2.0×10^3	3.2×10^{-3}	1,600	2.2×10^3	3.3×10^{-3}	1,500	2.3×10^3	3.4×10^{-3}	1,500
CD4 (phosphorylated)	3.0×10^3	3.0×10^{-3}	1,000	3.3×10^3	3.1×10^{-3}	940	3.5×10^3	3.0×10^{-3}	857

Table S2. Binding of purified AP2 and recombinant AP2 core complexes to sorting signals.

Synthetic peptides corresponding to the sorting signals of the indicated proteins were immobilized on a CM5 sensor surface of a BIAcore 3000 and probed for binding of AP2 purified from pig brain as well as recombinant AP2 core complexes, harboring a phosphorylated or nonphosphorylated Thr156 in the μ2 subunit. Binding of purified AP2 was comparable to that of the non-phosphorylated AP2 core, showing the functionality of the recombinant protein. Interestingly, binding to tyrosine sorting signals was enhanced by more than 10-fold upon phosphorylation of μ2 at Thr156, while the weak binding of the dileucine signals was almost unaffected.

Processing of sensorgrams recorded with a BIAcore 3000 biosensor

The binding of AP2 to membranes was recorded in real-time using a BIAcore 3000 biosenor as outlined in Experimental procedures. Before the rate constants for the interaction can be calculated, the original data set has to be processed adequately, which is outlined in the figure below.

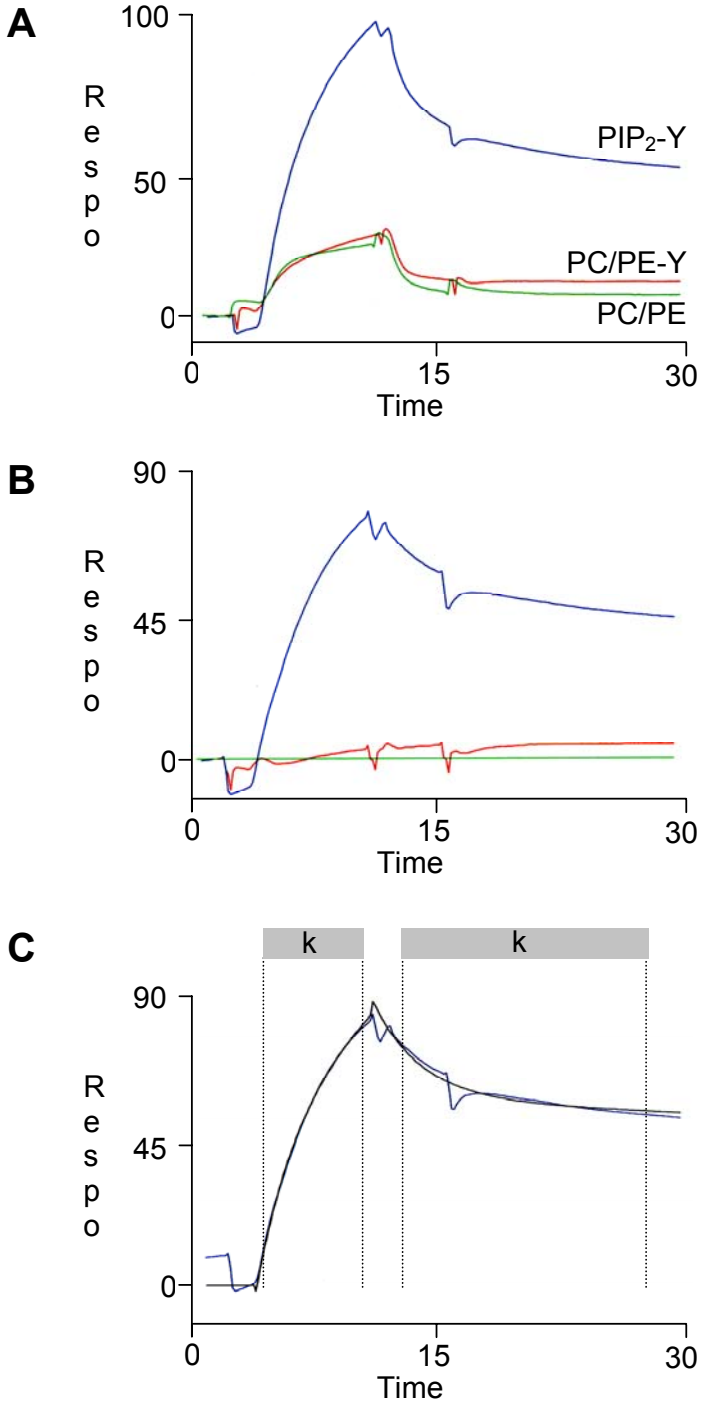

Figure S2
In **A**, the original data set of binding of recombinant AP2 (non- phosphorylated core) to the 3 indicated surfaces is shown. All 3 sensorgrams were recorded simultaneously in real-time. **B**: After data acquisition, binding of AP2 to membranes containing PC/PE which was regarded as background binding was substracted from the other two sensorgrams by using the evaluation software supplied by the manufacturer. This resulted in a flat line for PC/PE and a curve very similar to it for PC/PE-Y. Thus, binding of AP2 to PC/PE-Y is negligible. **C:** After background substraction, the indicated areas of the remaining curve were selected for calculating the rate constants of the interaction (k_a and kd). The calculation was done by using a mathematical model that assumes 2 binding sites in AP2 for membranes. The significance of the calculated data was verified by superimposition of a theoretical curve (black) with the curve obtained in our experiment (blue). As shown, both curves exhibit a high degree of identity. The visible distortions in the original curve are due to valve switching at the beginning an end of the injection of AP2 that become visible when one of the central parts of the BIAcore biosensor (the integrated fluid cartridge, IFC) reaches the end of its live time.

Fingerhut, A., K. von Figura, and S. Honing. (2001). Binding of AP2 to sorting signals is modulated by AP2 phosphorylation. *J Biol Chem*. 276:5476-82.
Jonsson, U., L. Fagerstam, B. Ivarsson, B. Johnsson, R. Karlsson, K. Lundh, S. Lofas, B. Persson, H. Roos, I. Ronnberg, and et al. (1991). Real-time biospecific interaction analysis using surface plasmon resonance and a sensor chip technology. *Biotechniques*. 11:620-7.